

AUTUMN COLLEGE ON PLASMA PHYSICS

25 October - 19 November 1999

Examples of the Non-Local Self-Organization in the Heliosphere

Igor Veselovsky

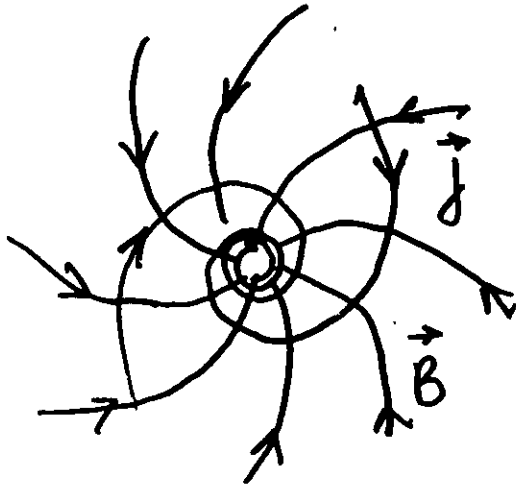
Institute of Nuclear Physics
Moscow State University
Russia

These are preliminary lecture notes, intended only for distribution to participants.

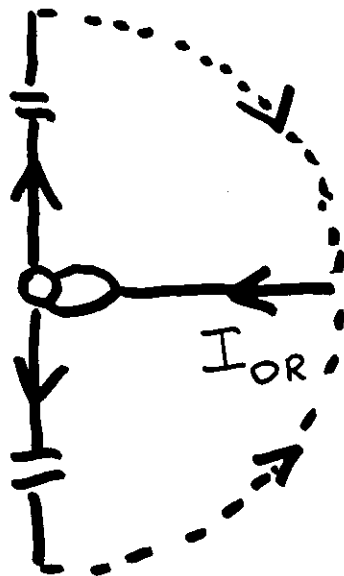
Contents

1. Fields and currents in the heliosphere	1
2. Field-aligned currents	8
3. Solar wind vortex flow	22
4. Nonstationary electric drifts	26
5. Induced electric fields	28
6. On the energy and momentum transport by the stable and unstable plasma waves	35
7. Ray approximation	40
8. Shock front geometry	49
9. Bow shock associated electric currents (BSEC)	54
10. Open, closed and intermittent magnetic structures	58

Fields and currents in the heliosphere



double
layers



H. Alfvén. (1979, 1981)

$$I_{OR} \sim 3 \cdot 10^9 \text{ A}$$

$$I_{\varphi} \sim 200 I_R$$

(Veselovsky, 1994)

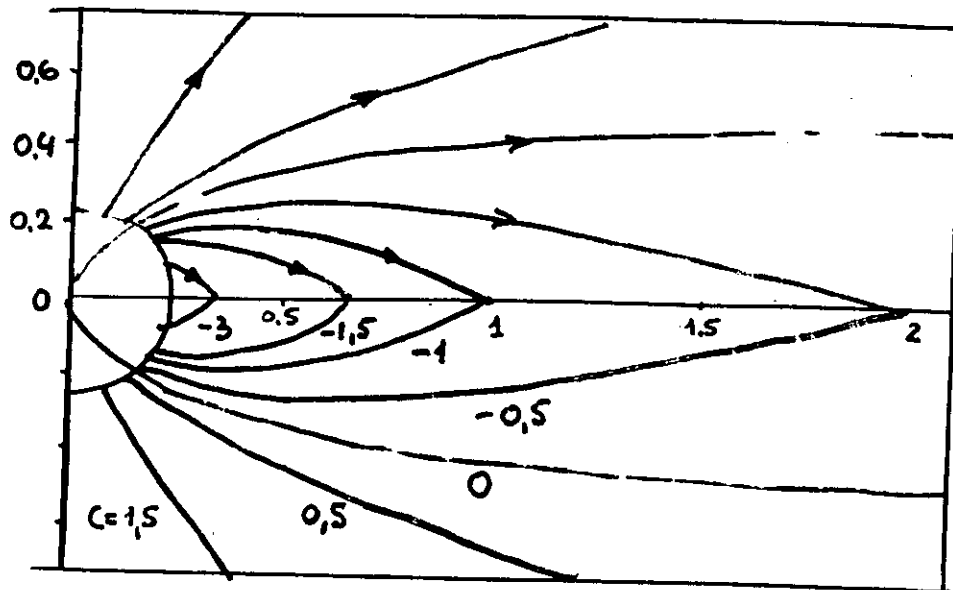
Model

declining phase and solar minimum : $\theta = \pi/2$
 point dipole \vec{M} + thin equatorial ring
 current $d\varphi \sim r^{-3}$

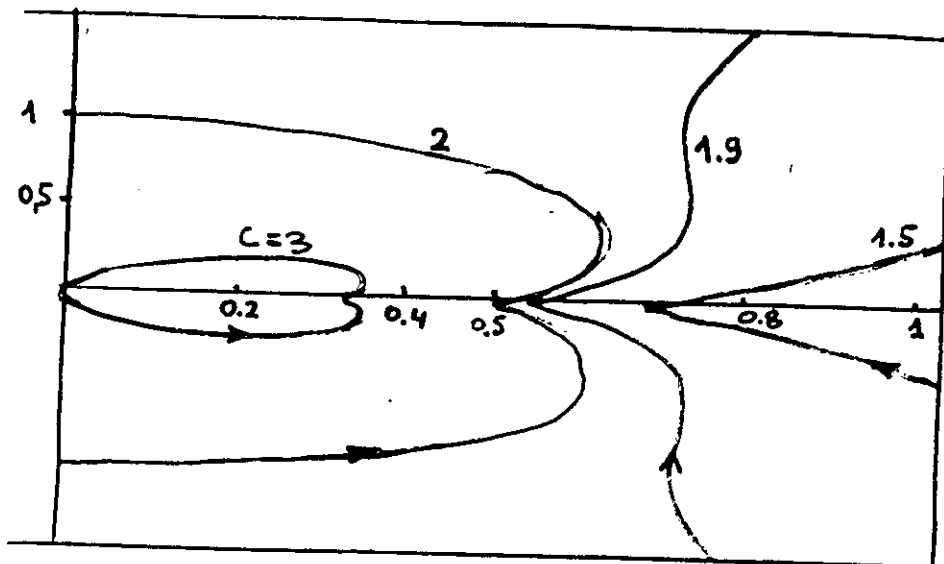
correct asymptotics $\uparrow r \rightarrow 0$

$\uparrow r \rightarrow \infty$

$|B_r(\theta)| = \text{const}$
 Ulysses



$a < 0$



$a > 0$

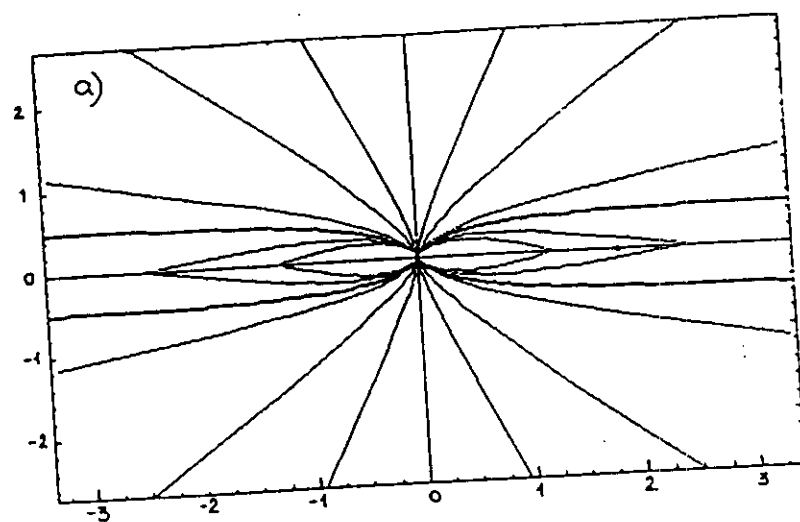
$$B_r = 2Mr^{-3}\cos\theta + B_0\left(\frac{r_0}{r}\right)^2\text{sign}(\theta - \pi/2)$$

$$B_\theta = Mr^{-3}\sin\theta$$

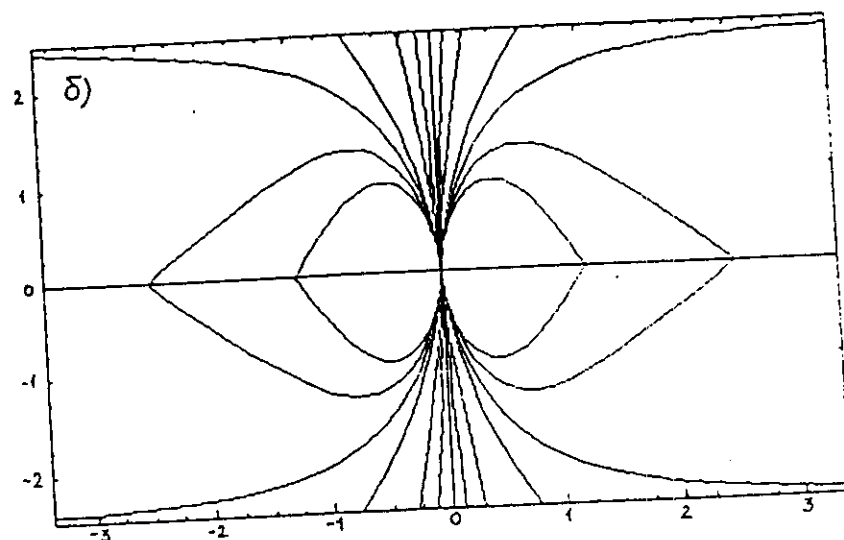
$$\Phi = B_0 r_0^2, \quad a = 2M/\Phi, \quad \rho = r/a$$

$$\rho = \sin^2\theta (C - 2|\cos\theta|) - \text{field lines} \quad (6)$$

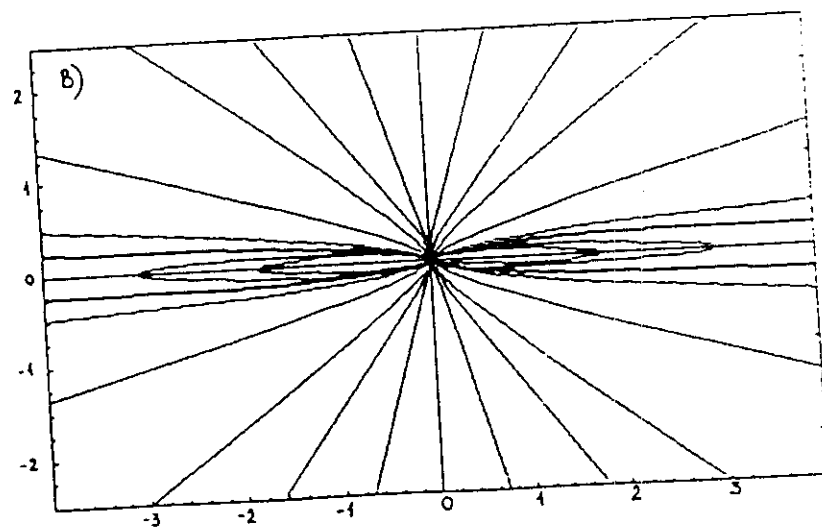
$a \sim 1$



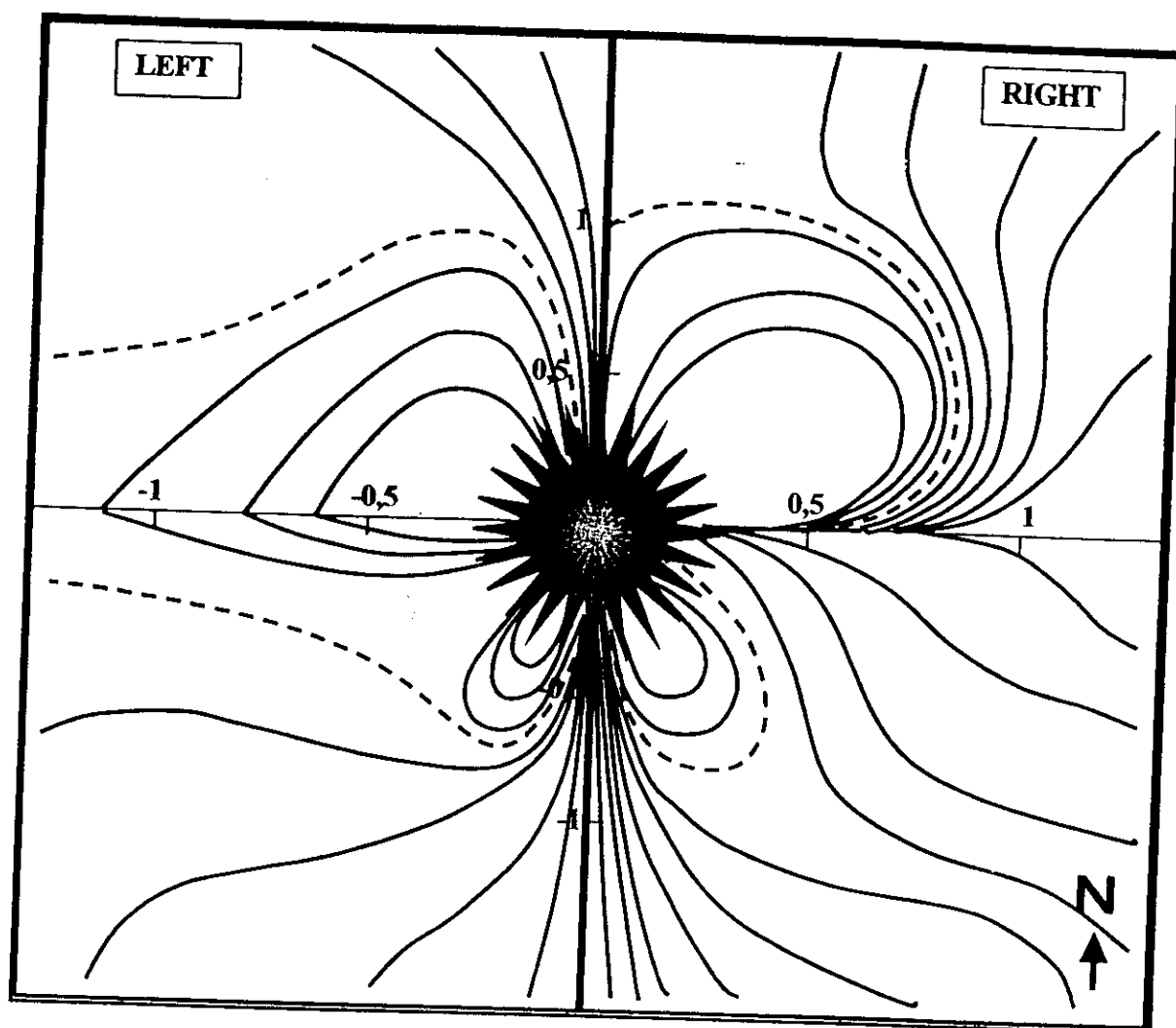
$a \rightarrow \infty$
 $\Phi \rightarrow 0$



$a \rightarrow 0$
 $\Phi \rightarrow \infty$



Линии маг. поля



Слева: слага 3, $\mu \uparrow \uparrow \Phi$, $\kappa \downarrow \uparrow \mu$

Справа: слага 4, $\mu \uparrow \downarrow \Phi$, $\kappa \downarrow \uparrow \mu$

Left: dipole + current sheet - quadrupole

Right: dipole - current sheet - quadrupole

Heliospheric magnetic field lines \vec{B} and electric currents \vec{I} near the equatorial plane during solar minimum a) inner heliosphere ~ 1 AU; b) outer heliosphere

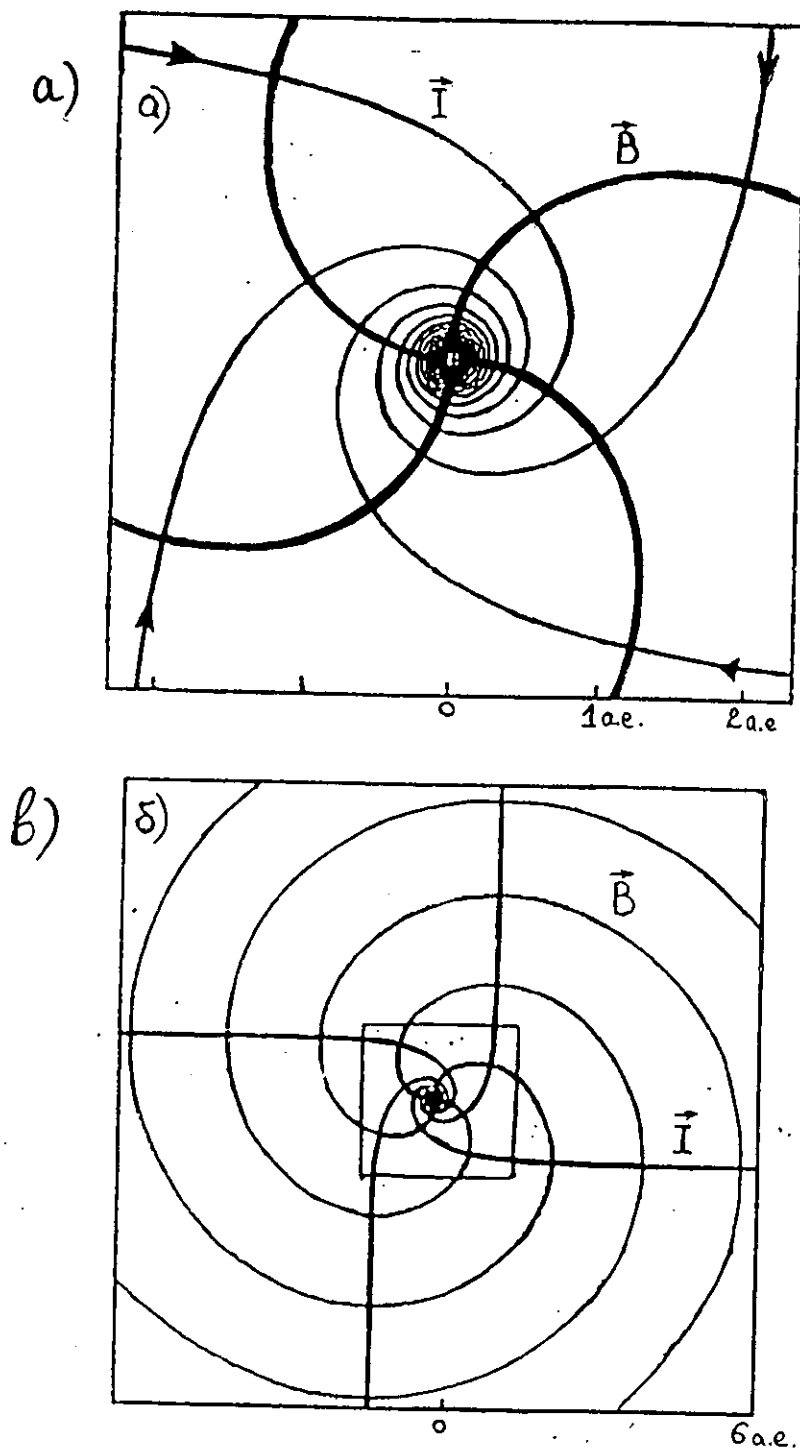


Рис.21 Конфигурации линий межпланетного магнитного поля (ММП) в плоскости тонкого токового слоя и электроджетов, созданных этим ММП в плоскости гелиоэкватора: а) во внутренней гелиосфере; б) во внешней гелиосфере.

Fig. 4 represents the configuration of the heliosphere when the rotational axis of the Sun is perpendicular to the axis of the main solar dipole ($\alpha = \pi/2$, $\beta = \pi/2$). In the equatorial cross-section ($z = 0$) the field line equation in dimensionless variables with the scale length L reads

$$\frac{dv}{dx} = \frac{[y - gx(x^2 + y^2)^{1/2}] \operatorname{sign}(\cos \gamma)}{[x + gy(x^2 + y^2)^{1/2}] \operatorname{sign}(\cos \gamma) + (x^2 + y^2)^{3/2}}. \quad (9)$$

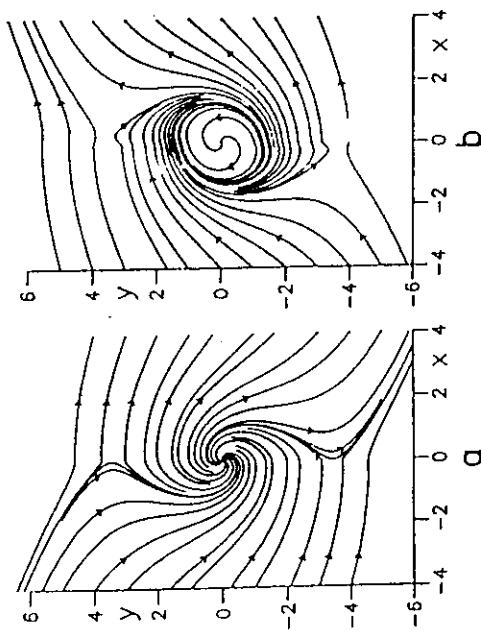


Fig. 4. Qualitative pattern of equatorial cross-section of the magnetic field structure corresponding to the model shown in Fig. 2; the field line equation is given by (9) with $g = 3.44$. The rotation axis of the Sun is perpendicular to vectors B_0 , μ_1 ; a) ($E_0\mu_1 < 0$), b) ($E_0\mu_1 > 0$).

Right-handed Cartesian coordinates are used with the z axis along the rotation axis of the Sun and the x axis along B_0 . Here $g = \Omega L/v$, and $\cos \gamma = \cos(\varphi_\mu - \varphi)$.

Figures 3 and 4 are calculated for $B_1 = 5$ nT, $B_0 = 0.5$ nT, $r_0 = 1$ A.U., $v = 400$ km/s, and Ω given by the sidereal rotation of the Sun. Fig. 4 probably corresponds to the period of the main solar dipole reversal after solar cycle maxima [7]. At this time, orientations a) to c) may occur during one solar rotation. However, for these periods the dipole approximation does not appear sufficiently good [8].

In solar cycle minima, the dipole axis is close to the rotation axis of the Sun; the qualitative pattern of reconnection for $B_0 \perp \Omega$ and B_1 model given in Fig. 2 is shown in Fig. 5. In this case $\alpha = 0$, $\beta = \pi/2$, $\gamma = \Theta$, and the magnetic field structure in the outer heliosphere is given by the sum of B_* (3) and B_0 .

The field line equation in dimensionless coordinates may be written as

$$dx/dy = gy[-gx + (x^2 + y^2 + z^2)^{1/2} \operatorname{sign} z]^{-1}, \quad (10)$$

where again $g = \Omega L/v$.

around the solar rotation axis. The condition $B_r = 0$ yields

$$r = L[-\cos \Theta \cos \beta \operatorname{sign}(\cos \gamma)]^{1/2},$$

where

$$L = r_0(B_1/B_0)^{1/2}$$

and $B_\varphi = 0$ yields

$$r = b \sin \Theta \operatorname{sign}(\cos \gamma) [\sin \beta \sin(\varphi_B - \varphi)]^{-1},$$

where

$$b = \Omega L^2/v.$$

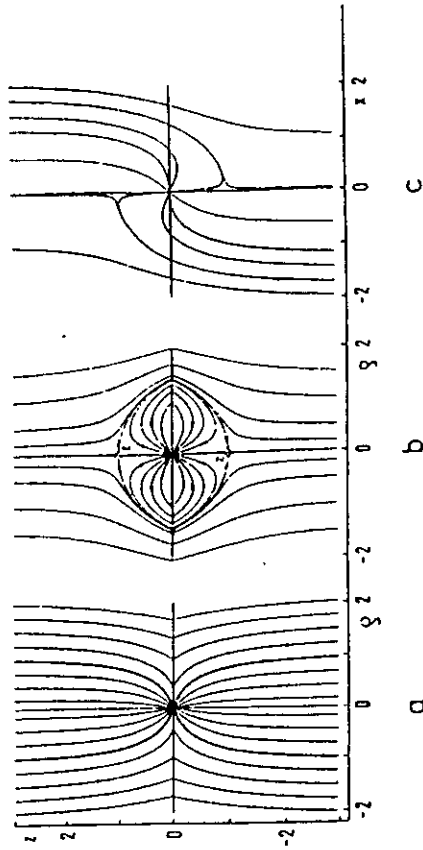


Fig. 3. Qualitative picture of the solar and interstellar magnetic field reconnection corresponding to the model given in Fig. 1; the field line equation is given by (8), $L = 3.16$ A.U. Solar rotation is not taken into account. a) ($E_0\mu_1 > 0$), b) ($E_0\mu_1 < 0$), c) ($E_0\mu_1 = 0$); $\gamma = 0$; Z zero points.

Fig. 3 shows a qualitative picture of the field line pattern for the solar magnetic field model given in Fig. 1, if the interstellar magnetic field is acting a) parallel, b) antiparallel and c) perpendicular to the field of the main solar dipole.

In dimensionless variables, using the scale length $L = r_0(B_1/B_0)^{1/2}$,

$$\begin{aligned} \text{a) } dq/dz &= q[z + (z^2 + z^2)^{1/2} \operatorname{sign} z]^{-1} \\ \text{b) } dq/dz &= q[z - (z^2 + z^2)^{1/2} \operatorname{sign} z]^{-1} \\ \text{c) } dx/dz &= x[z + (x^2 + z^2)^{1/2} \operatorname{sign} x]^{-1} \end{aligned} \quad (8)$$

where z, q are cylindrical and x, x Cartesian coordinates. Although this representation holds for a nonrotating Sun, it indicates the principal configurations.

In Fig. 4 a qualitative picture of magnetic field lines in the outer heliosphere is shown as obtained from the B_1 model given in Fig. 2. Decisive for the open or closed configuration is the component of the interstellar field which is parallel to the main solar dipole direction. The perpendicular component causes a shift of the field lines as shown in Fig. 3c.

Integrating (5), we obtain for every instant of time t a one-parameter set of field lines depending on parameter C (integration constant)

$$(6) \quad r = r_0 + Vt - (V/\omega) \arccos(C \sin^{-2} \Theta).$$

The pattern of projection of the magnetic field lines at a fixed moment is shown qualitatively in Fig. 1a. The projection of magnetic field lines (circle $r = r_0 + Vt + (\pi/2)(V/\omega)$) corresponds to the value $C = 0$. Along this circle, the radial component of magnetic field $B_r = 0$ is absent. Along circles $r = r_0 + Vt$, $r = r_0 + Vt + \pi(V/\omega)$, etc., on the contrary, the magnetic field projection shows a pure radial direction.

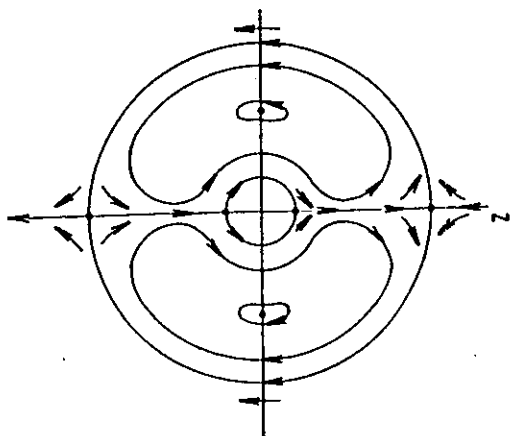


Fig. 1a. Schematic pattern of the IMF configuration in the meridional cross-section under non-stationary boundary condition (for changes of the dipole solar field).

The pattern of magnetic field lines is determined by the existence of a set of X-type zero points above the poles at distances $r = r_0 + Vt + (2n+1)(\pi/2)(V/\omega)$ from the centre, and those of the O-type at distances of $r = r_0 + Vt + n\pi(V/\omega)$ in the equatorial plane where $n = 0, 1, 2, \dots$. The evolution of the pattern of magnetic field lines is determined by the motion of the zero points in the radial direction away from the Sun. At the same time, on an arbitrary concentric surface that could be chosen as the starting one, new zero points and loops of the magnetic field are created continuously. The size of the loops then becomes larger, they move away from the Sun and disengage from the starting surface.

The closed magnetic configurations, originated in this way, move away from the Sun together with the moving plasma of the solar wind. Note that in the dynamic model, taking the influence of the magnetic field on the plasma motion into account,

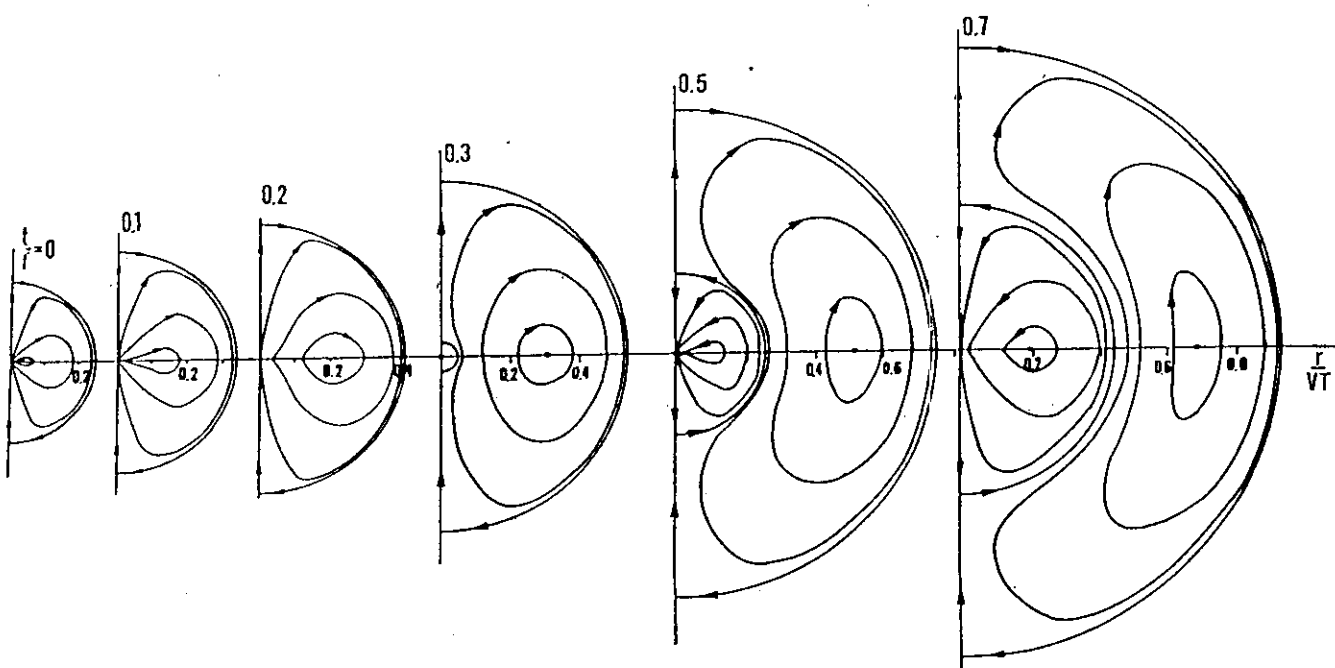


Fig. 1b. Projection of IMF lines onto the meridional plane at fixed time instants. The coordinate system is heliocentric, the z -axis points along the magnetic dipole axis depending on time as $\mu = \mu_0 \sin \omega t$. Results of calculations made for different time instants for $T = 2\pi/\omega \approx 2.5 \times 10^6$ s, $V = 400$ km/s, $r_0 = 7 \times 10^5$ km, $VT = 10^9$ km, $C \in \langle -1, 1 \rangle$ are presented. The time evolution of magnetic field lines is determined by the motion of the zero points radially away from the Sun, and by continuous formation of new structural elements near to the starting surface. The process of formation and motion of magnetic clouds away from the Sun in interplanetary space due to the effect of a constant solar wind and of variable solar magnetic field can be seen.

FIELD-ALIGNED ELECTRIC CURRENTS IN THE HELIOSPHERE

I.S.Veselovsky

Institute of Nuclear Physics, Moscow State University, 119899, Moscow, Russia
phone: +7(095)939 1298; fax: +7(095)939 3553; e-mail: veselov@dec1 npi.msu.su

October 30, 1999

Abstract

Theoretical considerations are presented of the nonlocal electromagnetic coupling in the heliosphere. Magnetic field line twisting and helicity estimates are discussed and possible relations to the coronal structures are indicated in their dependence on the space-time scales. Quasistationary field-aligned electric currents in the heliosphere are connected to the Sun. On open field lines they are closing at the heliospheric boundaries when providing the coupling between the termination shock, the heliopause and the corona. On the closed field lines, which are less numerous in the heliosphere, they are predominantly associated with the inhomogeneous heliospheric current sheet and propagating magnetic field discontinuities. Nonstationary field-aligned electric currents are always present and associated with propagating perturbations, especially nonlinear Alfvén waves and rotational discontinuities, when providing temporary electromagnetic links between the Sun and the interplanetary medium.

Key words: Solar corona; heliosphere; magnetic fields.

1 INTRODUCTION

Electric currents and magnetic fields in the heliosphere provide nonlocal connections between its different parts as well as the solar atmosphere, the Sun and the interstellar medium. H. Alfvén (1981) proposed in 1977 the simple conceptual model of electric currents in the heliosphere, which was elaborated later (Veselovsky 1994, 1996a). The electromagnetic fields in the heliosphere are

multi-scale and complicated in space and time. The interplay between different scales is not always clear, but the tendency to form field-aligned structures is well known in many instances. The purpose of this paper is to describe the origins and the role of the electric currents along the magnetic field, i.e. the field-aligned currents in the heliosphere.

2 FIELD-ALIGNED PLASMA STRUCTURES IN THE SOLAR WIND FORMATION RE- GION AND THE HELIOSPHERE

Field-aligned density, velocity, temperature, heat flux, electric current enhancements and rarefactions in the solar corona appear due to the plasma and the magnetic field self-organization processes because of the free (mainly electromagnetic) energy available here. The situation is typical for open nonlinear systems with the energy, momentum and mass flows through them. It is well known that all plasma inhomogeneities tend to be field-aligned in the sufficiently strong magnetic fields. They are considered as good tracers of the magnetic field lines in the solar atmosphere and are often used to "visualize" the magnetic field geometry which is sometimes force-free. Both dissipative and nondissipative mechanisms are operative in producing field-aligned propagating and convective structures.

Numerous rays, loops, jets and more complicated structures tracing the magnetic fields in the solar atmosphere and especially in the corona are produced by dissipative processes and the ideal plasma instabilities under the influence of the available free energy. Corresponding dimensionless parameters allow to delimit many possible regimes in the solar atmosphere and the heliosphere (Veselovsky, 1996b). Based on this scaling analysis one general statement can be done: the ideal plasma approximations (inviscid flows, frozen magnetic fields etc.) could be used with the caution and only for sufficiently large scale structures and fast processes. The deviations from these approximations are not negligible in many instances in the solar atmosphere and the heliosphere. The smallest quasi-stationary entities are always strongly dissipative. They are responsible for many fine structures observed in the solar plasma and are competitive in this sense with propagating waves.

Dissipative phenomena are playing the decisive role in these self-organization processes at sufficiently small scales. The formation of the field aligned inhomogeneities takes place more or less independent on the initial and boundary conditions in many important situations only because of the anisotropy introduced by the presence of the magnetic field. This anisotropy is rather strong in

the solar atmosphere especially in the rarefied regions. All transport coefficients are tensor quantities here with larger components along the field. Because of this all dissipative (sufficiently small scale) structures tend to have elongated shapes along the magnetic field.

To illustrate this tendency, let us consider for example a point-like or some other perturbation (a fluctuation) of the ion concentration at some initial time moment. This fluctuation could be initiated by the internal or external driving forces. The following time evolution of this perturbation is described by the corresponding Green function of the governing equations (dissipative MHD or kinetic ones). For the simplest geometries this Green function may be written explicitly. The physical result is well known: the plasma diffusion process across the magnetic field is suppressed in comparison with the "free" diffusion along the field in the ratio of the mean free path length to the ion Larmor radius. This ratio is increasing with the height in the solar atmosphere. The "pencil-like" concentration inhomogeneities appear as a consequence of the evolution even for round-shaped initial inhomogeneities. The limitation processes for this tendency are also working and they could be related to other plasma and electromagnetic scales.

In the similar way as the anisotropic diffusion produces field-aligned density inhomogeneities, the anisotropic viscosity leads to the formation of the sufficiently small scale field-aligned velocity fluctuations (jets). Elongated temperature inhomogeneities appear in the same way because of the anisotropic heat conductivity. Heat fluxes and electric currents are structured according to the anisotropic heat conductivity and the electric conductivity. An example of the nondissipative process leading to the field-aligned structuring will be considered later (polar plume formation). Electric and magnetic fields are important drivers of this process and we consider them first of all.

In summary, field aligned structures in the heliosphere can be of different physical nature: dissipative or not dissipative, quasistationary or essentially time-dependent and propagating.

3 ELECTROMAGNETIC FIELDS AND THEIR SOURCES IN THE HELIOSPHERE

Electric fields in the heliosphere are connected with the free electric charges (potential electric fields) or time variable electric currents associated with alternating magnetic fields (induction electric fields). The electric fields are expressed through the scalar potential ϕ and the vector potential \vec{A} according to the

definition

$$\vec{E}(\vec{r}', t) = -\vec{\nabla}\phi - \frac{1}{c} \frac{\partial \vec{A}(\vec{r}', t)}{\partial t}. \quad (1)$$

Potentials are related to the electric charge density ρ and electric current density \vec{j} by the volume integrals according to the formulae

$$\phi(\vec{r}, t) = \int \rho(\vec{r}', t) R^{-1} d^3 r', \quad (2)$$

$$\vec{A}(\vec{r}, t) = \frac{1}{c} \int \vec{j}(\vec{r}', t) R^{-1} d^3 r', \quad (3)$$

where $R = |\vec{r} - \vec{r}'|$.

Potential electric fields and electric charges are sometimes a priori neglected or underestimated without sufficient grounds (see e.g. Cowling 1953, 1957; Dungey 1958) based only on the estimates for frozen-in conditions, which are not always fulfilled in the solar and space plasmas. The limited validity of the ideal plasma conductivity approximation is well known and was stressed many times by H. Alfvén. In the application to the overall heliospheric current circuit this means the unavoidable existence of double electric layers, which are still not sufficiently investigated in the heliosphere (Alfvén 1981). Probably these potential jumps exist not only in polar regions as was initially anticipated, but this problem remains open. Detailed measurements in the regions closer to the Sun where the dissipation is more important could give needed information about their existence, spatial distribution and parameters.

The local charge densities and the electric current densities are uniquely determined and can be calculated by the local differentiation of the fields or potentials when they are known as functions of their variables. In this sense the fields and potentials are more fundamental physical quantities than charges and currents, which also can be used to determine fields and potentials nonlocally by volume integrals (2,3).

The relative importance of potential and induced electric fields can be estimated using equations (1-3) as follows. Let us consider the dimensionless number $F = \frac{j}{\rho c} \frac{r}{ct}$ where characteristic values of the charge density, the electric current density, the space scale and the time scale are combined. The value F could be termed as Faraday number because it indicates that induction electric fields dominate when $F \gg 1$. This happens when electric currents are strong, time variable and the considered plasma volumes are sufficiently large. This situation is well investigated in the solar physics.

In the opposite case, when $F \ll 1$, the electrostatic charging dominates over the electromagnetic induction. The charging of the solar and space plasma is

poorly known and not appreciated. Nevertheless, it should be very important. The steady state situation dominated by the induction electric field is impossible. The only possible steady state should be dominated by the potential electric fields. It is clear from this consideration, that the plasma behaviour at the largest times could not be correctly described if even small charging is present, but neglected a priori. Deviations from the plasma neutrality and the charge separation effects are known inside thin layers and small cavities with the non-maxwellian plasma. Strong Langmuir waves and oscillations as well as other electrostatic modes and their manifestations in the particle distribution functions (accelerated particles and other deviations from the Maxwellian shape) should be searched in the solar and heliospheric plasma especially in the perturbed conditions, closer to the Sun and far from the equilibrium.

It is interesting to note the following definition of the "plasma" concept: "plasma is the system of charged particles with the total electric charge equal to zero and with the charge separation scale length much less than the dimensions of the system" (Frank-Kamenetskii 1968). According to this definition, there is no sense to use the term "plasma" in the opposite situation, but other authors still use the term "plasma" in a broader context even in this case. We conclude, that both extreme situations are present in the solar and space plasmas. The domains where electrostatic charging is essential in the heliosphere deserve more attentive investigation taking into account their principal physical role.

Magnetic fields in the electrically conducting medium are produced by the conductivity currents, convective currents and displacement currents. It is well known, that displacement currents are essential only for fast electrodynamic processes (waves). The conductivity currents dominate in the plasma in many instances but not always. Sometimes electric currents are transported by the convection of the charged fluid. It is possible to indicate a dimensionless number $Q = \frac{n_c v}{n v_d}$ which can be used to delimit the situations dominated by the conductive or convective electric currents. Here $n_c = \frac{\rho}{e}$ is the excess number density of the positive particles, v is the hydrodynamical velocity, n is the plasma number density, v_d is the relative drift velocity between positive and negative particles. The conductive current is dominant when $Q \ll 1$. This is the common situation because of good plasma quasi-neutrality. The convective current is dominant when $Q \gg 1$. This possibility is less investigated (charged fluid) and it is not known in applications to the heliosphere.

4 HELICAL STRUCTURES

Helical, kinked, sheared, twisted and more complicated writhed and linked structures in the solar atmosphere are very common. They are indicative of electric

currents. Formal mathematical definitions of the local and global geometry properties of the nonpotential fields can be found in the literature. Different point and integral quantities are sometimes named by the same term "helicity", referring to the presence, strength and the direction of electric currents. The simplest definition of the helicity for the given field \vec{A} is $(\vec{A}[\vec{\nabla} \times \vec{A}])$. It is a local not normalized helicity which represents the combined geometry and power characteristics of the field. The normalized local helicity is given by the expression $(\vec{A}[\vec{\nabla} \times \vec{A}])(|\vec{A}||\vec{\nabla} \times \vec{A}|)^{-1}$. This quantity varies between (-1,1) and represents the local property of the field geometry. The left spirals correspond to -1, and the right spirals to +1. The volume integrals of these local characteristics define global helicities. Other global quantities like the number of turns around the axis (so called twist), linkings, etc. are also represented as integrals.

The Faraday's relations between magnetic fields and electric currents allow to interrelate these different definitions of the magnetic helicity. The magnetic field \vec{B} is given by the vector potential \vec{A} according to the definition

$$\vec{B}(\vec{r}, t) = [\vec{\nabla} \times \vec{A}(\vec{r}, t)]. \quad (4)$$

Let us consider first of all local helicities. The vector potential helicity $(\vec{A}\vec{B})$, the magnetic field helicity $(\vec{B}\text{rot}\vec{B})$ and the electric current helicity $(\vec{j}\text{rot}\vec{j})$ are connected each to other because of the Maxwell equations, the relation

$$\vec{A}(\vec{r}, t) = \frac{1}{4\pi} \int [\vec{B}(\vec{r}', t) \times \vec{R}] R^{-3} d^3 r', \quad (5)$$

and the Bio-Savart law:

$$\vec{B}(\vec{r}, t) = \frac{1}{c} \int [\vec{j}(\vec{r}', t) \times \vec{R}] R^{-3} d^3 r', \quad (6)$$

where $\vec{R} = \vec{r} - \vec{r}'$. The relation (6) is valid for quasistationary fields when displacement currents are negligible in comparison with conductivity and convection electric currents \vec{j} . If it is not the case, the displacement current $\frac{1}{4\pi} \frac{\partial \vec{B}(\vec{r}', t)}{\partial t}$ appears and this additional term should be retained together with the current \vec{j} in equation (6). It is seen that the field-aligned current density is very important ingredient in any case.

Field-aligned electric currents in the polar regions are responsible for the formation of the helical structures which are seen from times to times in polar plumes (Veselovsky et al. 1999). The helical angle is rather small and indistinguishable in many instances, but sometimes attains values of 30-40 degrees. Field-aligned electric currents produce transversal nonradial magnetic fields which strongly affect the local transport processes inside and around the plumes. The rough order of magnitude estimates of the electric current per each plume give values

of several $10^9 A$. These currents are presumably closing the global electric circuit in the heliosphere which is formed in the essential measure by the partial azimuthal ring currents of the streamers inside the main heliospheric current sheet and the transient convective and propagating current sheets associated with shock waves and discontinuities (Veselovsky et al.1999).

Much stronger electric currents (up to $\sim 10^{11} - 10^{12} A$ by the order of magnitude) are associated with the main heliospheric current sheet especially with its parts nearest to the Sun. The heliospheric current wedge restructuring because of internal and external causes can be associated with eruptive events. Eruptive events like prominences and coronal mass ejections often appear as complicated multi-scale phenomena containing helical structures clearly seen during the active phase initiated by the electric current changes. The helicity of the more stable configurations seems to be not so pronounced.

We refer to the papers (Veselovsky 1994,1996a) for the details of the heliospheric electrojet models and the global magnetic field configuration in the solar wind formation region. The possibility of the intermittent closure currents inside the heliosphere was not taken into account in the initial concept of the equivalent quasistationary current system with all closure currents between low and high heliolatitudes supposed to be concentrated exclusively at the heliopause (Alfven 1981). We suggest the modified concept of the equivalent current system which seems to be more realistic in comparison with previous constructions. The branching ratio between different meridional currents in the heliosphere, at its boundaries and in the interstellar medium need additional investigations and should be solar cycle dependent.

5 ESTIMATES OF THE DISSIPATION IN THE SOLAR ATMOSPHERE

It is well known that the Joule dissipation is concentrated at different places under different boundary conditions. It is concentrated at the places of the maximal electrical conductivity, where maximal current densities exist under the conditions of a given electric field intensity (parallel shunting). It is concentrated at the places of the minimal conductivity, where maximal electric fields exist under the conditions of a given electric current strength (consecutive chain). Both situations are known in the solar atmosphere. The global electric circuit in the system "Sun-heliosphere-interstellar medium" encompasses the regions with different physical parameters, but the lowest temperatures and field-aligned conductivities ($\sigma \sim T^{-3/2}$) are met in the solar atmosphere. Because of this, the main Joule dissipation occurs here.

Let us consider in brief toroidal and poloidal electric currents in the heliosphere (Alfven 1981, Veselovsky 1994). The strongest toroidal electric currents in the heliosphere are associated with the permanent existence of the magnetic field sector structure and the radial magnetic field component with the intensity independent on the angular coordinates on the sphere around the Sun. These toroidal currents are concentrated near the Sun in the heliospheric current sheet with the surface current density $\sim r^{-2}$ and its continuation inside the streamer belt around filaments and prominences with more complicated geometry of current distributions. The integral current strength is about $\sim 10^{11} - 10^{12} A$ by the order of magnitude. The quasi-stationary part of this current is of a drift nature and dissipationless. The alternating part is of the same order of magnitude according to the interplanetary magnetic field measurements. This part penetrates deep in the solar corona and dissipate the energy via Joule heating and viscous friction in moving circuit elements. The effective potential drop along this current loop can be estimated as follows $2\pi \frac{v}{c} B_{\odot} R_{\odot} \sim 10^{11} V$. The magnetic energy stored by this current is of the order of $\frac{B_{\odot}^2}{8\pi} R_{\odot}^3 \sim 10^{27} J$. This free energy is sufficient to feed even the most powerful events like coronal mass ejections on the Sun and represents their upper limit. The existence of such a limit indicates on the important role of the free energy accumulation and recuperation inside the corona. The power needed to support this alternating current against the dissipation is of the order of $\sim 10^{22} W$. This power is sufficient to cover the total energy losses by the solar corona provided by the heat conduction, the electromagnetic radiation and the solar wind outflow acting together in different proportions depending on locations and the solar cycle phase. The geometry of this current loop is rather simple and quiescent during the solar minimum years, but it is much more complicated and dynamical during solar maxima. The parts of this loop nearest to the Sun play their role in the coronal mass ejections processes from the global and biggest events with energies of $10^{26} - 10^{27} J$ up to the smallest and indistinguishable transients distributed in the energy according to the turbulent power laws.

The electric field in the heliosphere in the reference frame fixed to the moving solar wind in the region beyond the solar wind source surface $\vec{E}' = \vec{E} + \frac{1}{c}[\vec{v} \times \vec{B}]$ is small because of the high electrical conductivity, $E' = 0$. The frozen-in-conditions are approximately valid here. They are stronger violated in the regions where the conductivity is the lowest, i.e. near the Sun. The tangential (horizontal) electric field is continuous on the solar wind source surface and below this surface in the solar atmosphere. The flow velocity is negligible here, $v = 0$ and the horizontal electric field "penetrates" to lower levels in the solar atmosphere from the upper levels in heliosphere where it is supported by the solar wind induction. Hence, $\vec{E} = -\frac{1}{c}[\vec{v} \times \vec{B}]$, $\vec{j} = \sigma \vec{E}$, are good zero order approximations at the levels below the solar wind source surface (for simplicity we neglect at the moment the tensor properties of the conductivity, $j_i = \sigma_{ik} E_k$).

Horizontal electric currents tend to be field-aligned in the given electric field because of higher conductivities along the magnetic field. The high conductivity channels are formed self-consistently as in nonlinear percolation problems with given boundary conditions. The maximal dissipation $jE = \sigma E^2$ takes place in these "current channels" with maximal effective conductivities which are tracing the magnetic field geometry. The interplay between the local and the global geometry could explain the diversity of the visual shapes in the solar corona. Unfortunately, the sensitivity of the photospheric magnetic field measurements is not sufficient to measure the presence and the structure of the global horizontal and vertical magnetic fields (several Gauss) on the Sun produced by the heliospheric current sheet. We conclude that external (heliospheric) electric fields and currents are essential in the solar corona in many respects.

Poloidal electric fields and currents are driven by the unipolar induction of the rotating Sun (see e.g. Alfvén and Fälthammar 1963). The characteristic order of magnitude estimates of the electric field potential are $\sim 0,1GV$, the electric current $\sim 1GA$, the dissipated power $\sim 10^{17}J$, which is too small in the global balance. Some remarks are in order about the magnetic field geometry. Horizontal magnetic fields are relatively small in the coronal holes. Because of this, the horizontal electric fields are also small. The horizontal magnetic fields are strongest in the active regions. This means that induced electric fields and currents are strongest here. The difference between the dissipation level in coronal holes and active regions is also mediated by the conductivities which are dependent on the temperature and the magnetic field geometry. Simplest geometries correspond to the homogeneous approximation in the box with given boundary conditions. More complicated situations correspond to the one-scale inhomogeneity in the box. The real solar situations are multi-scale and three dimensional ones. We mention the possibility to have locally field-aligned but globally cross-field structures. An illustrative example: the real inhomogeneous heliospheric current sheet. Another possible situation: globally field-aligned but locally cross-field structures. This situation is not known in the heliosphere. We have considered mainly the Joule dissipation, which is locally important and provided by field-aligned currents. The viscous dissipation seems to be not less important and may be even the dominant mechanism in the overall coronal heating, but it is related to the electric currents across the magnetic field accelerating the plasma elements by the Ampere force.

6 POLAR PLUME FORMATION PROCESS

Let us consider the nondissipative process of the field-aligned structure appearance due to the electric drifts in the time dependent magnetic field in the solar atmosphere. Nonstationary electric fields are especially important in erupting

prominences, rising and shrinking coronal loops (Veselovsky 1998). The corresponding process is also associated with the polar plume formation on the tops of ephemeral magnetic regions under some appropriate conditions on the Sun (Veselovsky et al. 1998).

Ephemeral magnetic regions in the photosphere represent bipolar magnetic structures with different orientations and characteristic values of $B_1 \sim 10 G$, time scale $t \sim 3 \cdot 10^4 s$ and space scales $b \sim 10 Mm$. They generate induced electric fields $E \sim 0,3 V/m$ according to the Faraday's law

$$\vec{E}(\vec{r}, t) = -\frac{1}{4\pi c} \int \left[\frac{\partial \vec{B}_1(\vec{r}', t)}{\partial t} \times \vec{R} \right] R^{-3} d^3 r', \quad (7)$$

where $\vec{R} = \vec{r} - \vec{r}'$.

Induced electric fields (7) bring the plasma in a drift motion across the magnetic field with the velocity

$$\vec{V}_\perp = c \frac{[\vec{E} \times \vec{B}]}{B^2}. \quad (8)$$

The magnetic field consists of several parts according to partial electric currents of the model representation.

In our analytical model we assume $\vec{B}(\vec{r}, t) = \vec{B}_0 + \vec{B}_1(t)$, where \vec{B}_0 is the global quasistationary magnetic field in polar regions given with a good accuracy for the low activity phase of the solar cycle by the superposition of the point dipole placed in the center of the Sun and the thin heliospheric current sheet in its equatorial plane, see [Ves96a]. Global magnetic field lines in this model are described by the formula

$$\rho = \sin^2 \Theta (C - 2 |\cos \Theta|)^{-1}, \quad (9)$$

where $\rho = r/a$ - dimensionless heliocentric distance, $a = 2\mu/\Phi$ - characteristic length, μ - magnetic dipole of the Sun, $4\pi\Phi$ - open magnetic flux of the Sun, θ - polar angle, $C > 0$ - arbitrary constant serving as a parameter for open field lines in polar regions.

The part \vec{B}_1 represents potential fields of the ephemeral magnetic region assumed for the simplicity to be a time-dependent point magnetic dipole $\vec{\mu}_1(t)$ on the photosphere. This lowest order approximation is sufficient for our purposes to demonstrate the role of nonstationary electric drifts, but in reality a more complicated geometry and underlying magnetic field structures obviously could exist.

With these assumption, drift velocities are estimated from (8) and (7) as follows

$$v_\perp (km/s) \sim 10^3 \left(\frac{B_1}{B} \right) \left(\frac{r_\perp}{t} \right), \quad (10)$$

where $r_{\perp}(Mm)$ is the characteristic scale across the magnetic field and $t(s)$ is the corresponding duration time. For $r_{\perp} \sim b \sim 10 Mm$, $t \sim 3 \cdot 10^4 s$, $B_1 \sim B$ we obtain from (4) an estimate $v_{\perp} \sim 0,3 km/s$. The drift is subsonic and sub-alfvenic.

The simplest geometry which allows a detailed analytical treatment corresponds to the paraxial approximation near the poles with the vertical $\vec{\mu}_1(t)$. This axially symmetric case with vertical time-dependent magnetic fields and azimuthal induced electric fields was investigated. The results are described below.

The time-dependent magnetic configuration $\vec{B}(\vec{r}, t)$ in this case is rather simple and contains separators and zero-points at distances about $\sim \left(\frac{\mu_1}{B_0}\right)^{1/3}$, which are larger but comparable to b and determine the space scale r_{\perp} of the phenomenon.

The continuity equation for the plasma density n

$$\frac{\partial n}{\partial t} + \nabla(n\vec{v}) = 0 \quad (11)$$

was approximated as

$$\frac{\partial n}{\partial t} + \nabla_2(n\vec{v}_{\perp}) = 0 \quad (12)$$

or

$$\frac{\partial n}{\partial t} + \frac{(nv_l)}{\partial l} = 0 \quad (13)$$

depending on the ratio $\varepsilon = \frac{v_l}{v_{\perp}} \frac{r_{\perp}}{l}$ between the velocities and scales along and across the magnetic field.

Compressions or rarefactions of the density on the given field line appear because of the drifts (8) according to equation (12), which is valid for $\varepsilon \ll 1$. It is easy to see that $\text{div}_2(n\vec{v}_{\perp}) < 0$ and $\frac{\partial n}{\partial t} > 0$ if $\frac{\partial n}{\partial l} > 0$. This result corresponds to the "frozen-in condition" in the cylindrical case (6). We suppose that the approximation $\varepsilon \ll 1$ is a reasonable one in the lower parts of plumes where $v_l \ll v_{\perp}$. Further out from the Sun, in the main body of the visible plumes, $\varepsilon \sim 1$ because of the solar wind formation and $v_l \gg v_{\perp}$, $r_{\perp} \ll l$ here. Finally, at the tops, where the supersonic solar wind formation is mostly completed, $\varepsilon \gg 1$ and the approximation of thin tubes (7) is applicable.

Momentum balance equations for the plume formation process are written in a standard form

$$nm_p \left(\frac{\partial v_{\perp}}{\partial t} + v_{\perp} \frac{\partial}{\partial r_{\perp}} v_{\perp} \right) = - \frac{\partial p}{\partial r_{\perp}} + \frac{1}{c} j_{\varphi} B_l, \quad (14)$$

$$nm_p \left(\frac{\partial v_l}{\partial t} + v_\perp \frac{\partial v_l}{\partial r_\perp} + v_l \frac{\partial v_l}{\partial l} \right) = \frac{\partial p}{\partial l} - \frac{M_\odot m_p G n}{r^2}, \quad (15)$$

$$v_\varphi = 0, \quad (16)$$

where m_p is the proton mass. The energy balance equation is substituted by the assumption $T = \text{const}$ for simplicity and because of our poor knowledge of the real energetics, which may be complicated. The justification for the assumption of nearly isothermal conditions with slow coronal motions was given in the literature, see [Parker58 and Parker63]. The detailed analysis of equations (8,9) is rather complicated and will not be reproduced here, because it is more or less irrelevant for the main ideas of this paper about the dominant role of inductive electric fields for the phenomenon under consideration. It should be mentioned only that equation (8) determines transversal pressure balance conditions. The term $-\frac{1}{c} j_l B_\varphi$ is less important and was omitted in this equation. Equation (9) describes trans-sonic flows along thin flux tubes and was studied in many papers on the solar wind theory.

The solution show that for the initial development phase of a plume, when $\frac{\partial B}{\partial t} > 0$, $v_\perp < 0$, $\frac{\partial n}{\partial t} > 0$ and the linear time dependence of the magnetic field may be assumed, we have $n(t) = n_0 \exp \int (-\nabla_2 \vec{v}_\perp) dt$. The density exponentially increases with the characteristic time of the magnetic field, attains the observed maximal value which is several times higher than background values n_0 and stagnate when $\frac{\partial B}{\partial t} = 0$, $v_\perp = 0$. The plume decays, $\frac{\partial n}{\partial t} < 0$ when $\frac{\partial B}{\partial t} < 0$, $v_\perp > 0$.

Because of the continuity equation, each plume development is associated with the adjacent depletion region formation. Dark lanes $n < n_0$ appear at the sites where the local magnetic field initially decreases with time $\frac{\partial B}{\partial t} < 0$ and their evolution may be considered in a similar way. It is known for a long time that polar plumes are intermingled with dark lanes, see [Vsess65]. Our model explains this observational fact.

We conclude that polar plumes represent essentially nonstationary and three-dimensional MHD phenomenon driven by the electromagnetic induction. Time-scales and transversal space scales of ephemeral regions, XBPs and polar plumes are comparable, but the detailed one-to-one correspondence sometimes is obscured or lacking because of geometry conditions. Mutual angles between global fields, local ephemeral fields and viewing direction determine a large manifold of possibilities in this respect.

7 CONCLUSIONS

Field-aligned electric currents in the heliosphere are important in several aspects: 1) They represent the closure parts of the global electric circuit supported by the induced and potential electric fields. 2) They are also elements of the quasi-stationary self-organized force-free and pressure balanced structures as well as evolving helical convective inhomogeneities and propagating perturbations. 3) They participate in the energy transport between different domains in the heliosphere and provide the Joule dissipation in the solar atmosphere. 4) Often they appear as an immediate cause of instabilities and waves, but sometimes they are driven by waves or could be self-consistently adjusted to the situation depending on initial and boundary conditions. 5) They are related to the charge separation mechanisms responsible for the formation of the electric potential jumps and energetic particle acceleration. We conclude that field-aligned electric currents in the heliosphere play their role which needs additional quantitative investigation.

The work was partially supported by the Russian Foundation of Basic Research Grants 96-15-96710, 98-02-17660 and the State Program "Astronomy" Project 1.5.6.2. The author is grateful to the Local Organizing Committee for the support facilitating his attendance at the 9th European Meeting on Solar Physics "Magnetic Fields and Solar Processes".

References

- [Alfven 1963] Alfven H. and Falthammar C.-G., 1963, *Cosmical Electrodynamics*, Oxford, Clarendon Press
- [Alfven 1981] Alfven H., 1981, *Cosmic Plasma*, D.Reidel Publ. Co, Dordrecht, Holland
- [Cowling1953] Cowling T.G., 1953, in *The Sun*, G.P.Kuiper (ed.), The University of Chicago Press
- [Cowling1957] Cowling T.G., 1957, *Magnetohydrodynamics*, Interscience, New York
- [Dungey1958] Dungey J.W., 1958, *Cosmic Electrodynamics*, Cambridge
- [Frank-Kamenetskii1968] Frank-Kamenetskii D.A., 1968, *Plasma - the Fourth State of Matter*, Atomizdat, Moscow (in Russian)
- [Parker1963] Parker E.N., 1963, *Interplanetary Dynamical Processes*, Interscience, New-York
- [Parker1958] Parker E.N., 1958, *Astrophys. J.*, 128, 664-676
- [Veselovsky1994] Veselovsky I.S., 1994, *Geomagn. and Aeronomy*, 34, 45-51 (in Russian)

- [Veselovsky1996a] Veselovsky I.S., 1996a, Geomagn. and Aeronomy, 36, 1-7 (in Russian)
- [Veselovsky1996b] Veselovsky I.S., 1996b, Solar Wind Eight, AIP Press, Woodbury, New York, 161-164
- [Veselovsky1998a] Veselovsky I.S., 1998, New Perspectives on Solar Prominences, AIP Press, Woodbury, New York, 123-126
- [Veselovsky1998b] Veselovsky I.S., Panassenko O.A. and Koutchmy S., 1998, Solar Jets and Polar Plumes, ESA SP-421, 345-347
- [Veselovsky1999] Veselovsky I.S., Zhukov A.N., Koutchmy S., Delannee C. and Delaboudiniere J.-P., 1999, SOHO 8 Workshop (in press)
- [Vsesvjatskii et al.1965] Vsesvjatskii S.K., Nikolsky G.M., Ivanchuk V.I., Nesmjajovich A.T., Ponomarev E.A., Rubo G.A., Cherednichenko V.I., 1965, Solar Corona and Corpuscular Radiation in the Interplanetary Space, Kiev (in Russian)

Physics of the Outer Heliosphere.
Eds. S. Grzedzielski and D. E. Page.
Pergamon Press, Oxford, 1990. 277-280.

SOLAR WIND VORTEX FLOW IN THE OUTER HELIOSPHERE

I.S. Veselovsky

Nuclear Physics Institute, Moscow State University, Moscow, U.S.S.R.

ABSTRACT

The structure of the T. von Karman vorticity wake type near the heliomagnetic equator is considered. Linearized equations are used for polytropic gas on the background of axially symmetric supersonic flow with the velocity minimum at the equatorial plane in the heliosphere.

1. According to the contemporary ideas, the solar wind velocity increases with distance from the surface of the warped heliospheric current sheet. The existence of higher velocities of the flow at high heliolatitudes in years of solar activity minimum was established by radioastronomic data. The typical solar activity near the heliomagnetic equator are those of 400 km/s and far from it, 600-700 km/s in years of low solar activity. The free energy in this differential super-Alfven and supersonic motion is rather large and may cause the development of a wide spectrum of waves in the interplanetary plasma. More over nonstationary and inhomogeneous boundary conditions near the rotating Sun are also a source of perturbations propagating in the solar wind. Besides potential disturbances there may exist vortex motions. The below presented consideration was undertaken to investigate a regular structure of vortex streams in the solar wind with the smallest radial velocity. The result reminds a well known in hydrodynamics vortex wake behind a body flown around and qualitatively corresponds to the stream structure observed on board spacecrafts near the equatorial plane in the outer heliosphere /1-3/.

2. Let us consider the equations of motion of polytropic gas

$$\begin{aligned}\rho + \nabla(\rho \vec{v}) &= 0, \\ \rho [\vec{v} + (\vec{v} \nabla) \vec{v}] &= -\nabla p, \\ \dot{S} + (\vec{v} \nabla) S &= 0, \\ S &= p \rho^{-\gamma}.\end{aligned}\quad (1)$$

Let an axially symmetric radial expansion be in the zero approximation:

$$v_{\theta}(\theta) \text{ is the given function of polar angle } \theta \text{ independent of } r, \rho, \\ v_{\theta} = v_{\theta} = 0, \quad r^2 \rho v_{\theta} = \text{const}, \quad S = \text{const}.$$

For perturbation ρ_1, \vec{v}_1, p_1 one always has near $\theta = \pi/2$ in the local linear approximation:

$$\begin{aligned}\rho_1, \vec{v}_1, p_1 &\propto \exp i(kr - \omega t), \\ (\omega - kv_{\theta 0}) \rho_1 + ik \rho_0 v_{\theta 1} + \frac{2}{r} v_{\theta 0} \rho_1 + \left[(\pi/2 - \theta) \rho_0 v_{\theta 1} + \rho_0' v_{\theta 1} + \rho_0 v_{\theta 1}' \right] r^{-1} &= 0 \\ \rho_0 \left\{ -i(\omega - kv_{\theta 0}) v_{\theta 1} + \frac{v_{\theta 0}' v_{\theta 1}}{r} \right\} &= ik p_1.\end{aligned}\quad (2)$$

$$\rho_0 \left\{ -i(\omega - kv_{\lambda 0}) v_{\theta 1} + \frac{v_{\lambda 0}' v_{\theta 1}}{\lambda} \right\} = -\frac{p_1'}{\lambda}$$

$$-i(\omega - kv_{\lambda 0}) \rho_0^{-1} [p_1 - c_s^2 \rho_1] - \gamma v_{\lambda 0} \rho_0^{-1} \frac{\partial \rho_0}{\partial \lambda} [p_1 - c_s^2 \rho_1] - 2v_{\lambda 0} \rho_0^{-1} c_s \frac{\partial c_s}{\partial \lambda} \rho_1 - \frac{S_0' v_{\theta 1}}{\lambda} = 0.$$

Here the trait denotes differentiation over θ .

$$\rho_0 \approx \rho_0(\pi/2) + \frac{1}{2} \rho_0'' (\theta - \pi/2)^2.$$

$$v_{\lambda 0} \approx v_{\lambda 0}(\pi/2) + \frac{1}{2} v_{\lambda 0}'' (\theta - \pi/2)^2.$$

$c = (\gamma p / \rho)^{1/2}$ is the adiabatic sound velocity.

Let us examine now a fairly short-wave perturbation of the acoustic type $p_1 = c_s^2 \rho_1$, $v_{\theta 1} \sim \text{const} + o(\theta - \pi/2)$, $k\lambda \gg 1$ near $\theta = \pi/2$. The set of equations (2) can be rewritten as

$$-(\omega - kv_{\lambda 0}) \rho_1 + ik \rho_0 v_{\lambda 1} + \left[(\theta - \pi/2) \rho_0' v_{\theta 1} + \rho_0'' (\theta - \pi/2) v_{\theta 1} \right] = 0.$$

$$\rho_0 \left\{ i(\omega - kv_{\lambda 0}) v_{\lambda 1} + v_{\lambda 0}' (\theta - \pi/2) v_{\theta 1} \lambda^{-1} \right\} = ik p_1. \quad (3)$$

$$\rho_0 \left\{ (\omega - kv_{\lambda 0}) v_{\theta 1} \right\} = -\frac{p_1'}{\lambda}.$$

$$p_1 = c_s^2 \rho_1.$$

Perturbations $v_{\lambda 1}$, p_1 , $\rho_1 \propto (\theta - \pi/2)$ can be expressed through $v_{\theta 1}$:

$$p_1 = i(\omega - kv_{\lambda 0}) (\theta - \pi/2) \rho_0 v_{\theta 1}.$$

$$\rho_1 = c_s^{-2} p_1. \quad (4)$$

In the case when the angular width of a sheet occupied by a slow wind satisfies the condition $\alpha \ll (M k \lambda)^{-1}$, $M = v_{\lambda 0} / v_{TF}$ - the Mach's number for protons, v_{TF} being their thermal velocity. Eq. (3) yields

$$\omega = k (v_{\lambda 0} - v_{\lambda 0}' \frac{\rho_0'}{\rho_0}).$$

$$v_{\lambda 1} = \frac{i \rho_0'}{k \lambda \rho_0} (\theta - \pi/2) v_{\theta 1}. \quad (5)$$

If $k \lambda \alpha \gg 1$, the dispersion relation reads

$$\omega \approx k(v_{\lambda 0} \pm c_s) \quad (6)$$

and perturbations $v_{\lambda 1}$ and p_1 are expressed through $v_{\theta 1}$

$$v_{\lambda 1} = ik\lambda (\theta - \pi/2) v_{\theta 1},$$

$$p_1 = \pm ik\lambda \rho_0 c_s (\theta - \pi/2) v_{\theta 1}. \quad (7)$$

If $M^{-1} \ll k \lambda \alpha \ll 1$, then

$$\omega \approx kv_{\lambda 0} [1 - (k\lambda M \alpha)^{-2/3}] \quad (8)$$

The available imaginary parts prove to be of a higher order of smallness so strong instabilities in the local approximation are absent. Similar investigations of large-scale perturbations beyond the local approximation are still lacking.

3. Formulae (7) type driven by respective it, the qualitative system moving vortex with ze

Fig.1. The vortex st

At $\theta = \pi/2$ The o-type zero p located at th This distance the distance the centres there is a p propagating in "anticycl

4. It is of observations plane at dis changes (see to (7) and t attract att consideratic and v_{λ} , how to perturbat radial velo be seen. Th is equal to

Our linear motions in and the rol The role of pattern rem particular, at large di spacecrafts Sun's rotat smaller-sce

RI

1. A.J.L. wind and conference Colorado 1

2. A.J.L. U.Villante Preprint 9

Solar Wind Vortex Flow

3. Formulae (7) describe two sets of vortex perturbations ψ type driven by the stream with the velocity u upstream and downstream. ψ respectively it with the velocity u . The qualitative form of the summary field of velocities in the system moving with velocity u . This velocity field has the ψ vortex with zero points of two types.

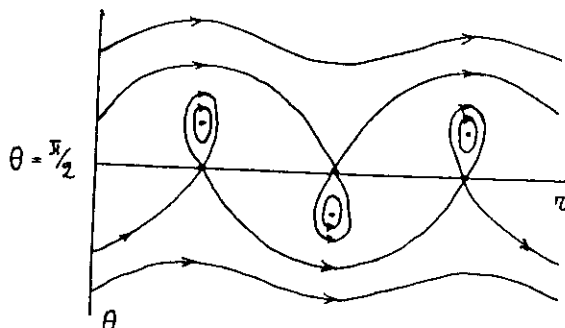


Fig.1. The qualitative pattern of a velocity field in the propagating vortex structures near the solar equatorial plane in the solar wind.

At $\theta = \pi/2$ The x-type zero points are observed, at some value of θ_{\pm} there are o-type zero points. The o-type zero points represent the vortex centres located at the distance $z = \pm 2k^2 v_{\theta 1} / v_{\theta 0} = (\theta_{\pm} - \pi/2) \lambda$ from the plane $\theta = \pi/2$. This distance can be seen to increase with the perturbation amplitude, with the distance from the Sun and with decreasing slope of the profile $v_{\theta 0}(\theta)$. At the centres of vortices propagating downstream (the sign "+" in (6), (7)) there is a pressure minimum as in "cyclones". At the centres of vortices propagating upstream (the sign "-" in (6), (7)) there is a pressure maximum as in "anticyclones".

4. It is of interest to compare qualitatively the results obtained with observations of oscillations in the solar wind stream near the helioequator plane at distances up to 25 a.u. /1,2/. Firstly, the correlated character of changes (see Fig.2 in /2/ and Fig.3 in /3/), having the same phase according to (7) and the period approximately equal to the Sun's rotation period attract attention. Secondly, in the "Voyager-2" spacecraft data under consideration one can also observe a correlated character of variation of v_{θ} and $v_{\theta 1}$, however changed strongly compared with a simple linear theory, due to perturbations being nonlinear. A rapid steepening of the fronts of the radial velocity and a large amplitude of density and pressure variations can be seen. The frozen-in magnetic field calculated in kinematic approximation is equal to $B_{\theta 1} = -B_{\theta 0} v_{\theta 1} / v_{\theta 0}$, where $B_{\theta 0}$ is the unperturbed spiral field.

Our linear gas-dynamic consideration indicates only the possibility of vortex motions in the solar wind. A more complete theory should regard nonlinearity and the role of the magnetic field as well as a real geometry of the flow. The role of these factors is discussed in /3-8/ however at present a real pattern remains insufficiently clear both in theory and observations. In particular, it is still partially unclear why the stream structure observed at large distances in the heliosphere on board the "Voyagers" and "Pioneers" spacecrafts seems to be simpler than at the Earth's orbit and comprises the Sun's rotation period as the main time scale, while near the Earth's orbit a smaller-scale structures are prevailing.

REFERENCES

1. A.J.Lazarus and J.Belcher, Large-scale structure of the distant solar wind and heliosphere, Proceedings of the sixth international solar wind conference, eds. V.J.Pizzo, T.E.Holzer and D.G.Sime, NCAR/TN-306 Boulder, Colorado 1988, v.2, p.533.
2. A.J.Lazarus, B.Yedidia, L.Villanueva, R.L.McNutt, Jr., J.W.Belcher, Villante and L.F.Burlaga, Meridional plasma flow in the outer heliosphere, preprint CSR-P-88-10, Cambridge, 1988.

Observations in the distant heliosphere: a view from Voyager

232

A.J. Lazarus and R.L. McNutt, Jr

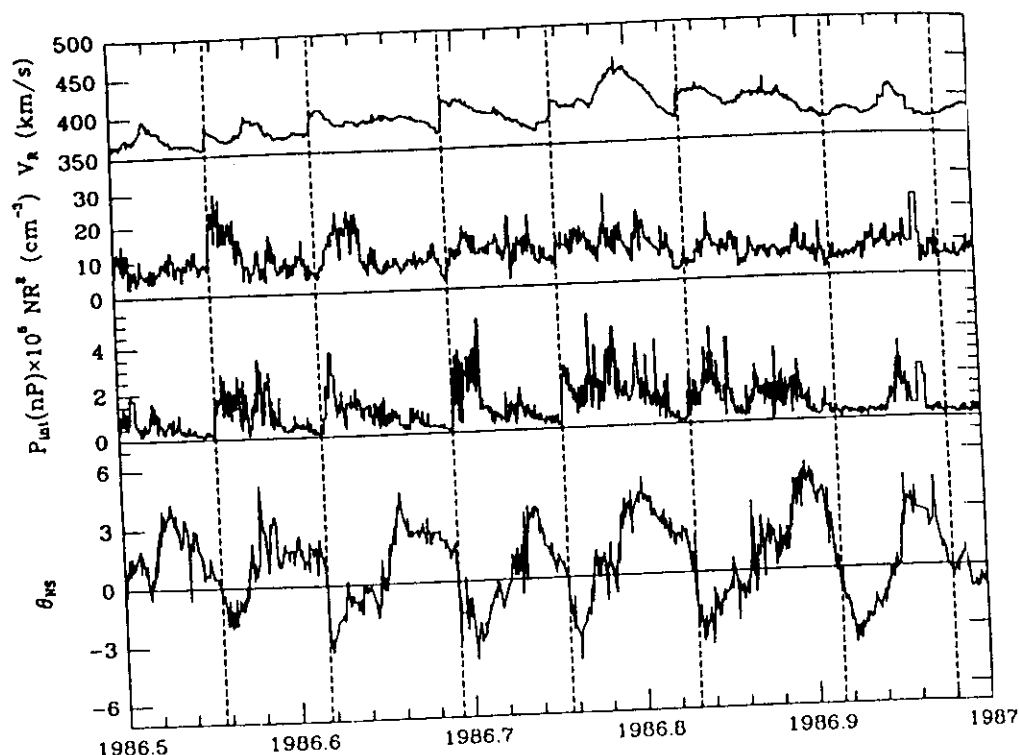


Fig. 4. 1-hour averages of Voyager 2 data taken near 25 AU. The vertical dashed lines indicate times of shocks. Note the great increase in number density accompanying the shocks. The internal pressure, P_{int} , shows the result of increases in temperature, density, and field strength. See [7] for more details.

Those interactions result in the formation of shocks that interact with shocks from adjacent streams [8]. The net effect is to produce regions of greatly varying number density and temperature. Those regions are responsible for the large variations in dynamic pressure seen in Figure 3; the pressure variations are due mainly to the large variation in density. Another effect can be seen in Figure 4: the variation of the meridional flow angle at the shocks, see [7] and [9]. The solar wind at 25 AU is not at all smooth and featureless, at least in the equatorial plane.

DISCUSSION

The consequence of these observations of ram pressure variations over the solar cycle is that, to first approximation, the heliopause and terminal shock should move in and out in response to the pressure changes. Figure 5 illustrates the location of the shock as a function of time, assuming that the interstellar pressure is 1.3×10^{-12} dynes cm^{-2} . To calculate the distance to the termination shock, R_{sh} , we equated the interstellar pressure (reduced by a factor of 1.13 to take account of residual pressure in the downstream flow [10]) to the ram pressure normalized to 1 AU divided by R_{sh}^2 .

At this Warsaw workshop, M. A. Gruntman [11] pointed out that such motion of the termination shock corresponds to a maximum speed of $\sim 20 \text{ km s}^{-1}$. That speed is of great interest since the estimated fast-mode speed in the interstellar medium is approximately that magnitude. Thus the question of whether the motion of the sun through the interstellar medium at $\sim 20 \text{ km s}^{-1}$ would result in the formation of an outer shock [12], has been supplemented by the suggestion of a dynamic interaction varying from subsonic to supersonic over the solar cycle.

200
150
100
50
0
SHOCK DISTANCE (AU)

Fig

The obser-
motion of
show (Fig
and temp
produce a
confrontin
correlated
the gener
Friedrichs

In the lon-
propagati-
terminatio
local son
months to
and may
solar rota
such as t

Whether
modelers
pressure
phase of
heliograp
an even

The wor-
and Gra
and the
stimulat

Physics of the Outer Heliosphere, Eds. S. Grzedzielski
and D. E. Page. Pergamon Press, Oxford, 1990. 229-234.

Nonstationary electric drifts in the solar atmosphere

Igor Veselovsky

Institute of Nuclear Physics
Moscow State University

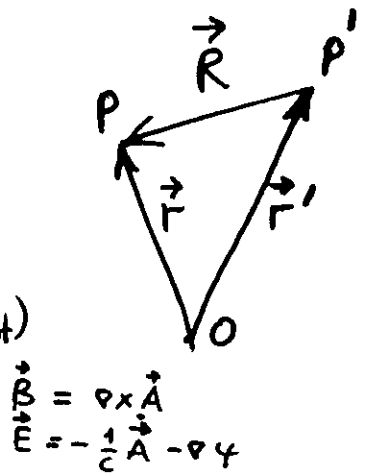
1. Induced electric fields

$$\text{rot } \vec{E} = -\frac{1}{c} \dot{\vec{B}}$$

$$\vec{E}(\vec{r}) = -\frac{1}{4\pi c} \int \frac{[\dot{\vec{B}}(\vec{r}') \times \vec{R}]}{R^3} d^3 r' \quad (+\vec{E}_{\text{pot}})$$

$$\vec{R} = \vec{r} - \vec{r}'$$

Faraday's law



2. Quasistationary fields

$$\text{rot } \vec{B} = \frac{4\pi}{c} \vec{j} + \frac{1}{c} \dot{\vec{D}} \quad (|\dot{\vec{D}}| \ll 4\pi \vec{j}, v \ll c)$$

$$\vec{B} = \frac{1}{c} \int \frac{[\vec{j}(\vec{r}') \times \vec{R}]}{R^3} d^3 r' \quad (+\vec{B}_{\text{pot}})$$

Biot - Savart law

3. Material equations (Ohm's law)

$$j_i = \sigma_{ik} (E_k - \frac{1}{c} \epsilon_{ikl} v_l B_l), \quad \sigma_{ik} = \sigma \delta_{ik}$$

$$\vec{j} = \sigma (\vec{E} - \frac{1}{c} [\vec{v} \times \vec{B}])$$

$$\vec{v}_\perp = c \frac{[\vec{E} \times \vec{B}]}{B^2} - \frac{c}{\sigma} \frac{[\vec{j} \times \vec{B}]}{B^2}$$

More complicated material equations (generalized Ohm's law)

Estimates

$$v_{\perp} \sim r/t.$$

Active region : $r \sim 10 - 100 \text{ Mm}$

$$v_{\perp} = 1 - 10 \text{ km/s} \quad \text{for } t \sim 10^4 \text{ s}$$

$$[(\text{km/s}) \quad v_{\perp} \approx 10^3 \tilde{N} r(\text{Mm}) t^{-1}(\text{s}),]$$

$$\text{where } \tilde{N} = \tilde{B}/B_{\text{tot}}, \quad B_{\text{tot}} = B_0 + \tilde{B}(t)$$

Drift velocities are increasing with the distance from the source of the magnetic perturbation.

Induced electric fields, X-ray bright points and plumes

I.S. Veselovsky
Institute of Nuclear Physics
Moscow State University

Purpose: polar plumes are related to
nonstationary magnetic fields and
induced electric fields

Introduction:

Q: Where plumes are anchored?

A:

- Spicules (^{1936 & 1941 eclipses} Bougaslarskaya, Vessviatsky 1941)

- Polar faculae (Waldmeier 1956)

- Chromospheric network (Pikelner 1962)

↑ Old times ← SOHO → New times ↓

- Unipolar magnetic footpoints

(C.E. DeForest & J.B. Gurman 1997 SOHO II)

- Polarity inversion lines

(P. Lamy et al. 1997 SOHO V)

- "Bright regions (magnetic dipoles) that flickers rapidly in time"

(K.R. Lang 1996 SOLTIP III)

EIT

Q: Why not 100% in the connection
BPR ^{K. Harvey} X BP — Plume ?

A:

↑
 $\frac{\partial B}{\partial t}$

↑
geometry

Because of time variability and
viewing conditions.

Essential elements in these comparisons:
 $\frac{\partial B}{\partial t}$, and orientations, projections

Induced electric fields and drifts

- Evolving small-scale bipolar regions in the photosphere (10G , $3 \cdot 10^4\text{s}$, 10Mm) generate induced electric fields

$$\vec{E}(\vec{r}, t) = -\frac{1}{4\pi c} \int \left[\frac{\partial \vec{B}}{\partial t} \times \vec{R} \right] R^{-3} d^3 r' \sim 0.3 \text{ V/m}$$

(Faraday's law) $\rightarrow \vec{E}_\perp$

Bottom

- Magnetic fields: $\vec{B}(t) = \vec{B}_0 + \vec{B}_1(t)$
 $a = \left(\frac{M}{B_0} \right)^{1/3}$ global $B_0 \sim 1\text{G}$
 local $B_1 \sim 10\text{G}$ - dipole $M(t)$

- Nonstationary electric drifts

$$v_\perp = c \frac{[\vec{E} \times \vec{B}]}{B^2} \sim 0.3 \text{ km/s}$$

- Density enhancements/rarefactions

$$\dot{\rho} + \vec{\nabla} \cdot (\rho \vec{v}) = 0$$

$$\dot{\rho} \approx -\vec{\nabla}_\perp \cdot (\rho \vec{v}_\perp)$$

- $(\vec{\nabla} \cdot \vec{E}) = 0$, given $E_\perp \rightarrow \vec{E}_\parallel$ geometry $(1:3)a$
- $E_\parallel \rightarrow$ field aligned currents
accelerated electrons (XBP)

Top

- field aligned currents are pinched

$$n_{\text{plumes}} / n_{\text{background}} > 1$$

$$\beta < 1 \quad (\text{nearly force-free})$$

$$\text{geometry } \frac{a}{l} : (2-3) : 10 \quad ?$$

viewing conditions

$$\vec{\nabla} \cdot \vec{v} = 0$$

$$\frac{\partial v_\parallel}{\partial t} = -\vec{\nabla}_\perp \cdot \vec{v}_\perp \rightarrow$$

- submagnetosonic flows $v_\parallel \sim v_\perp \frac{l}{a}$
 $v_\parallel \gg v_\perp$ if $l \gg a$

- magnetic flux ropes B_ϕ / B_θ

$\vec{B} = \vec{B}_0 + \vec{B}_1$
 external $\vec{J}_0 \rightarrow$ external ("potential") field \vec{B}_0

d_0

potential")

d_1

V

d_1

"nonpotential" part : \vec{B}_1

Dimensionless number $N = \frac{B_1}{B_0}$

1) $N \ll 1$ Strong external fields

(Syrovatskii S.I., 1969; Astrophys. Sp. Sci 4, 240

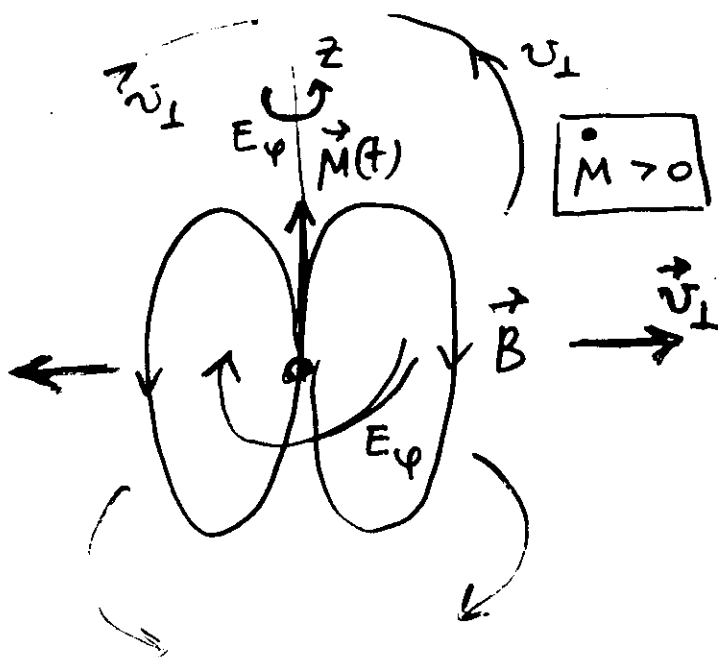
37 Gorbachev V.S. and Kellner S.R., 1988, Sov. JETP, 24, 89)

Filippov B.P., 1996, AIA, 313, 277

$$\vec{A} = \frac{\vec{M}(t) \times \vec{r}}{r^3}$$

20

Potential or force-free "zero approximation"



$$E_{\varphi} = -\frac{\dot{M}}{cr^2} \rightarrow v_{\perp} \sim \frac{r}{t}$$

plasma
condensations
are forming
on the pole. (

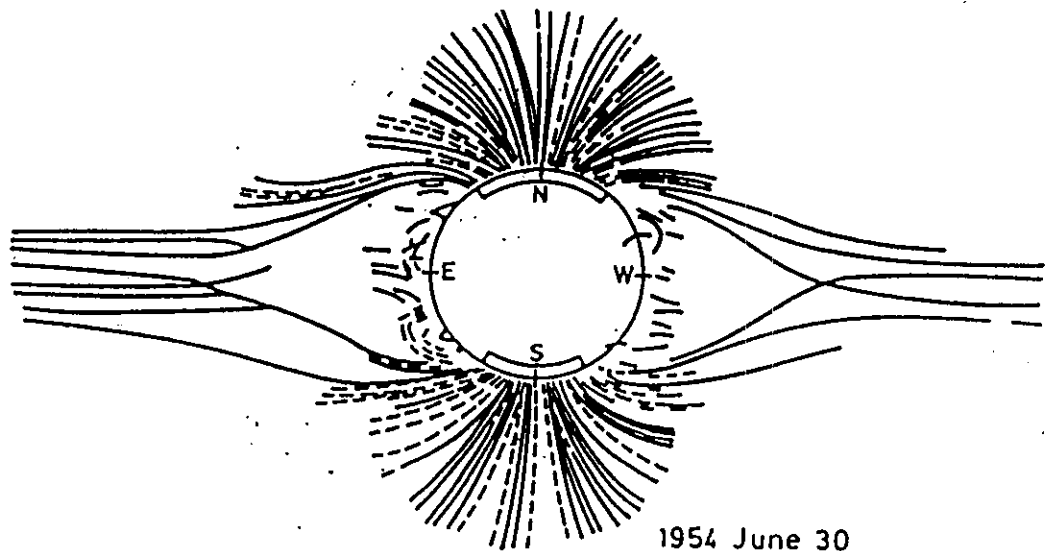
jets

$\dot{M} < 0 \rightarrow$ plasma condensations at the equatorial plane ("sheets")

"sheets"

2) $N \gg 1$

(Veselovsky I.S., 1996, Solar Wind 8, 171)



1954 June 30
($\phi = 0.04$; $R_z = 2.5$)

Figure 1. Structural drawing of the eclipse corona of June 30, 1954, made by the Kiev University group, from different plates. The latitude extension of polar coronal hole is drawn inside the disk. Note the asymmetry and the curvature or bending of a part of plumes. Rifts are observed where structures are drawn with dashed lines.

Shatten (1971) - current sheet model : open outside the source surface

Pneuman & Kopp (1971)
Pisanko (1985)
Linker & al (1990)] selfconsistent MHD streamer

X. Zhao & J. T. Hoeksema (1995) Horizontal current -
X.-M. Wang (1995) - current sheet model

Smith & al. (1995)
Burton & al. (1995)] Ulysses, $|B_r(\theta)| \approx \text{const}$

Axford & Gleeson (1976) - dipole + current sheet

North Polar Region

South Polar Region

K-cornua



FeX / X
(171 Å)



FeII
(195 Å)



FeIV
(284 Å)

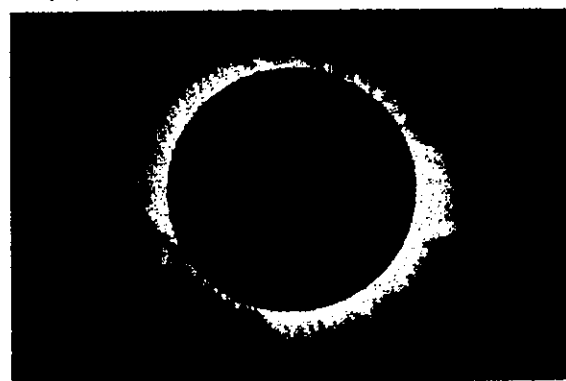




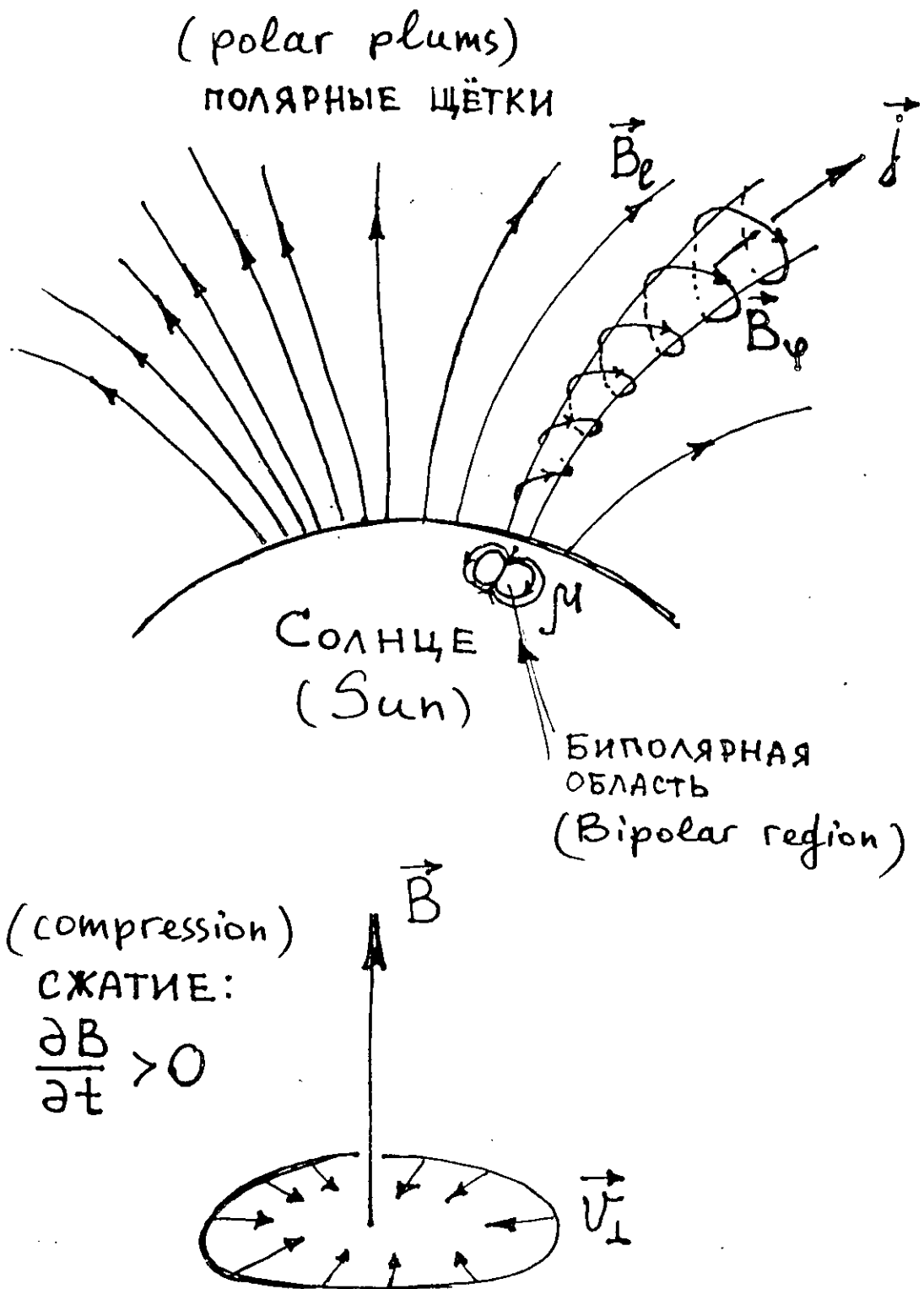
(B)



(C)



(D)



Development of the polar plume

Рис.20 Схема развития полярной щетки из нестационарной биполярной магнитной области.

On the energy and momentum transport by stable and unstable plasma waves in the solar corona and solar wind

(1)

I.S. Veselovsky

Institute of Nuclear Physics
Moscow State University
119899 Moscow Russia

Approach:

- Open system out of the LTE.
- Free energy for waves: inhomogeneity, nonstationarity of bulk parameters and other possible (kinetic) sources.

Result:

- The net effect: plasma heating/cooling acceleration/deceleration by growing, propagating and decaying waves depends on the initial and boundary conditions.

Usual suppositions:

- waves "from below"
- stability, dissipation
"maxwellian distribution function
(LTE)"

Equations:

(2)

$$\hat{\mathcal{D}} f = \frac{\partial f}{\partial t} + [\mathcal{H} f] = St$$

$$\hat{\mathcal{D}} = \hat{\mathcal{L}} + \hat{\mathcal{N}}$$

linear

nonlinear

$$\hat{\mathcal{L}} = \frac{\partial}{\partial t} + v_i \frac{\partial}{\partial x_i} + \frac{F_e}{m} \frac{\partial}{\partial v_i}$$

$$\hat{\mathcal{N}} = \frac{\hat{F}_i}{m} \frac{\partial}{\partial v_i}$$

external forces

internal forces
selfconsistent
Coulomb + Lorentz

↓ $[St]$:

- Conservation laws
 - number of particles
 - total momentum
 - total energy

MHD

Kinetics

Quasilinear theory

$$\hat{T} \bar{f} = 0$$

for resonant particles

propagation operator
for particles

averaged
distribution
function

$$(\gamma_k + \hat{A}_k) \varepsilon_k = 0$$

detriment

partial
wave energy

$$\gamma_k = B_k \frac{\partial \bar{f}}{\partial v}$$

linear (differential)
operator in t, \vec{r} space
(first order)

linear integral operator in
velocity space

Conservation laws for waves

- total momentum
- total energy

quasiparticle (plasmon) formalism

Simplest case: $\hat{A}_k = -\frac{1}{2} \frac{\partial}{\partial t} \rightarrow$

The energy of resonant particles
increases (decreases) in stable (unstable)
plasmas

The wave energy diminishes (grows)
when $\gamma_k < 0$ ($\gamma_k > 0$)

(4)

$\gamma = 0$: the interaction is switched off

↓ wave energy is conserved and the energy of particles is conserved too

Stationary waves does not accelerate the homogenous plasma (Washimi) 1981

Locally generated waves:

Free energy may be extracted from inhomogeneous flow.

→ deceleration or cooling

An example:

Radially expanding solar wind is unstable in the region of its subsonic flow where the formation of streams takes place

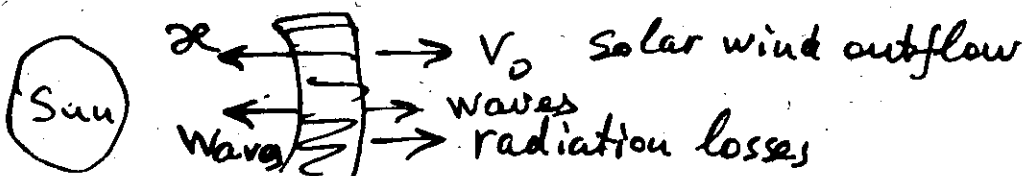
$$\gamma = - \left[\frac{v_0}{r} (v_0 r) \pm C_s \right] r^{-1} \quad (\text{Vexelovsky 1984})$$

$$v_0(r) < C_s$$

↑ sound speed

locally

Sound waves propagating inward are ~~unstable~~ and may regulate the thermal state of the solar corona together with the heat conductivity, and other mechanisms



Discussion:

(5)

1) WKB approximation is not sufficient:

$KL < 1$
is not fulfilled

(Molodykh 1988)
(Davila J.M. 1987)
(Suess S.T. et al. 1992)

2) Zero approximation ?

The splitting of the system on the "background" and "waves" is not clear in the fully nonlinear theory.

This is especially important when the (stationary) "background" does not follow from the solution of the initial or boundary problem.

Conclusion:

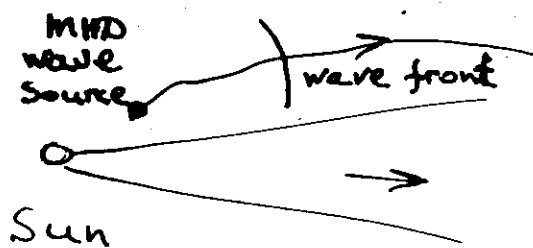
- "A successful wave theory has not yet emerged" (Hollweg)
- Acceleration/deceleration and heating/cooling depends on the distribution function shape
- The problem is selfconsistent in micro - and macroprocesses
micro - and macroscales
- Initial and boundary value problem to be solved.

Ray approximation for heliospheric MHD waves

Igor S. Veselovsky

Institute of Nuclear Physics
Moscow State University
Moscow 119899 Russia

1) Introduction : A ray concept



2) Heliosphere as a moving inhomogeneous medium for MHD wave propagation

3) Acoustogeometric phenomena in the heliosphere

- MHD wave modes
- wave energy transport
- refraction
- Mach surfaces
- dissipation and reverberation
- diffraction and dispersion
- linear, moderate, nonlinear

4) Conclusions

Generalized MHD vector of state

$$\vec{M} \{ \rho, \vec{u}, p, \vec{B} \}$$

← vector space $\vec{M}(\vec{r}, t)$

density velocity

pressure

obeys MHD (ideal or dissipative) equations

$$\hat{S} \vec{M}(\vec{r}, t) = 0 \quad (1)$$

nonlinear, nonstationary MHD operator: differential equations + boundary (initial) conditions.

Let us know the solution of Eq. (1):

$$\vec{M}_0(\vec{r}, t)$$

Let us consider a (linear) perturbation:

$$(\hat{S}_0 + \delta \hat{S})(\vec{M}_0 + \delta \vec{M}) = 0 \quad (2)$$

$$\hat{S}_0 \vec{M}_0 + \delta \hat{S} \vec{M}_0 + \hat{S}_0 \delta \vec{M} + \cancel{\delta \hat{S} \delta \vec{M}} = 0$$

$$0 = \delta \hat{S} \vec{M}_0 + \hat{S}_0 \delta \vec{M} = 0 \quad (3)$$

Linear equation

The solution:

$$\delta \vec{M} = - \hat{S}_0^{-1} \delta \hat{S} \vec{M}_0$$

The solver (inverse MHD operator)

$$\hat{S}_0^{-1} \hat{S}_0 = 1$$

$\sum_0^{-1} \rightarrow$ unperturbed characteristics

$$\delta \vec{M} = \sum_i e^{i\psi_i(r,t)} \delta \vec{M}_0$$

i - modes
fast
slow
Alfven

$$\frac{\partial \psi_i}{\partial t} + \left[\vec{v}(r,t) + c_i(r,t) \vec{n} \right] \cdot \frac{\partial \psi_i}{\partial \vec{r}} = 0$$

$$\boxed{\omega - k(v + c_i) = 0}$$

local
dispersion
equation

$$\boxed{\lambda \ll r, \omega t \gg 1}$$

Wave modes:

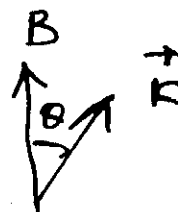
$$c_s = \sqrt{\gamma \frac{P}{\rho}} \quad - \text{Sound}$$

$$c_A = \sqrt{\frac{B^2}{4\pi\rho}} \quad - \text{Alfven}$$

$$c_I = c_A \cos \theta$$

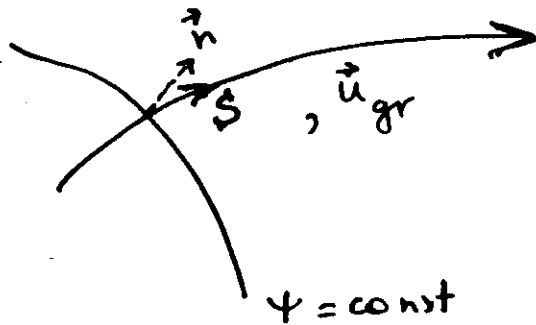
$$\theta = \pi/2 \quad c_M = \sqrt{c_A^2 + c_s^2} \quad \text{magnetosonic}$$

$$\theta = 0 \quad c_I \rightarrow c_A \quad \left\{ \begin{array}{l} \text{ent} \\ 2 \text{ Alfven} \\ \text{Sound} \end{array} \right.$$



$$\vec{n} = \frac{\partial \psi_i}{\partial \vec{r}} \left| \frac{\partial \psi_i}{\partial \vec{r}} \right|^{-1} = \frac{\vec{k}}{k} \quad - \text{phase front normal (Mach surface)}$$

Ray trajectory



$$\vec{s} = \frac{\vec{u}_{gr}}{|\vec{u}_{gr}|} = \frac{c\vec{n} + \vec{v}}{\sqrt{v^2 + c^2 + 2cv(\vec{n}\vec{v})}}$$

$$\vec{s}(\vec{n}, \vec{v})$$

$$\vec{n} = \vec{s} \left[\sqrt{1 + (\vec{s}\vec{v})/c - v^2/c^2} + (\vec{s}\vec{v})/c \right] - \vec{v}/c \quad \vec{n}(\vec{s}, \vec{v})$$

\vec{n} (phase normal) } does not coincide when $v \neq 0$
 \vec{s} (ray trajectory)

Propagation time along the ray $\int \frac{ds}{u_{gr}}$

- 1) Subsonic acoustics / solar corona /
 $v \lesssim c$
 $c_s < v < v_A$
 Acceleration
- 2) Supersonic acoustics / solar wind /
 $v > c$

↓
 Kinematics

Phase velocity

$$\vec{u}_{ph} = \frac{\vec{k}}{k} \left(\frac{\omega}{k} \right) = [c + (\vec{n} \cdot \vec{v})] \vec{n}$$

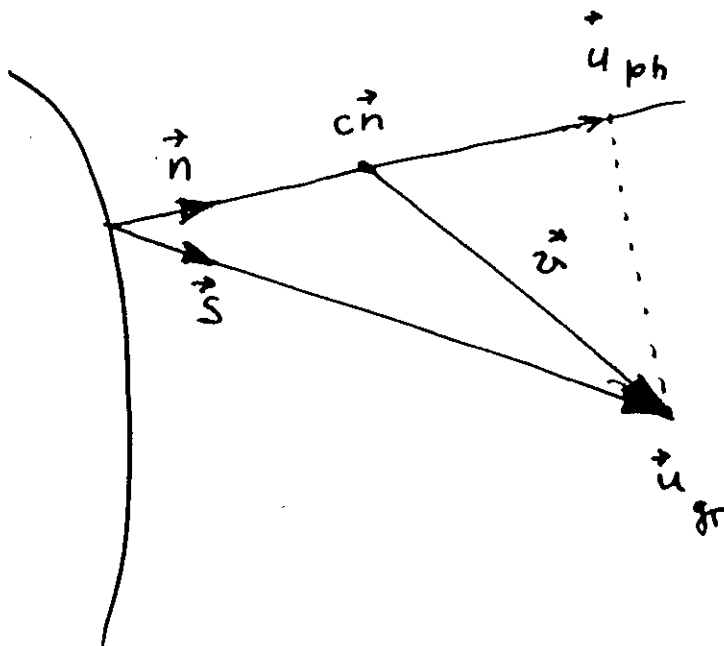
↑
definition

Group velocity

$$\vec{u}_{gr} = \frac{\partial \omega}{\partial \vec{k}} = \vec{v} + c \vec{n}$$

↑
definition


$$|\vec{u}_{ph}| = (\vec{n} \cdot \vec{u}_{gr}) = c + (\vec{n} \cdot \vec{v})$$





$\psi = \text{const}$
phase front


An example:


Convex, concave and hyperbolic Mach surfaces
in the heliosphere

• Sun  Convex (usual)

• Sun  concave (unusual)
high heliolatitudes?
HCS?

• Sun  hyperbolic?
HCS? inclination?

• Sun  equatorial
cross-section

• Sun  meridional
cross-section

Local shock geometry:

- Local heliospheric inhomogeneities
- Source geometry:

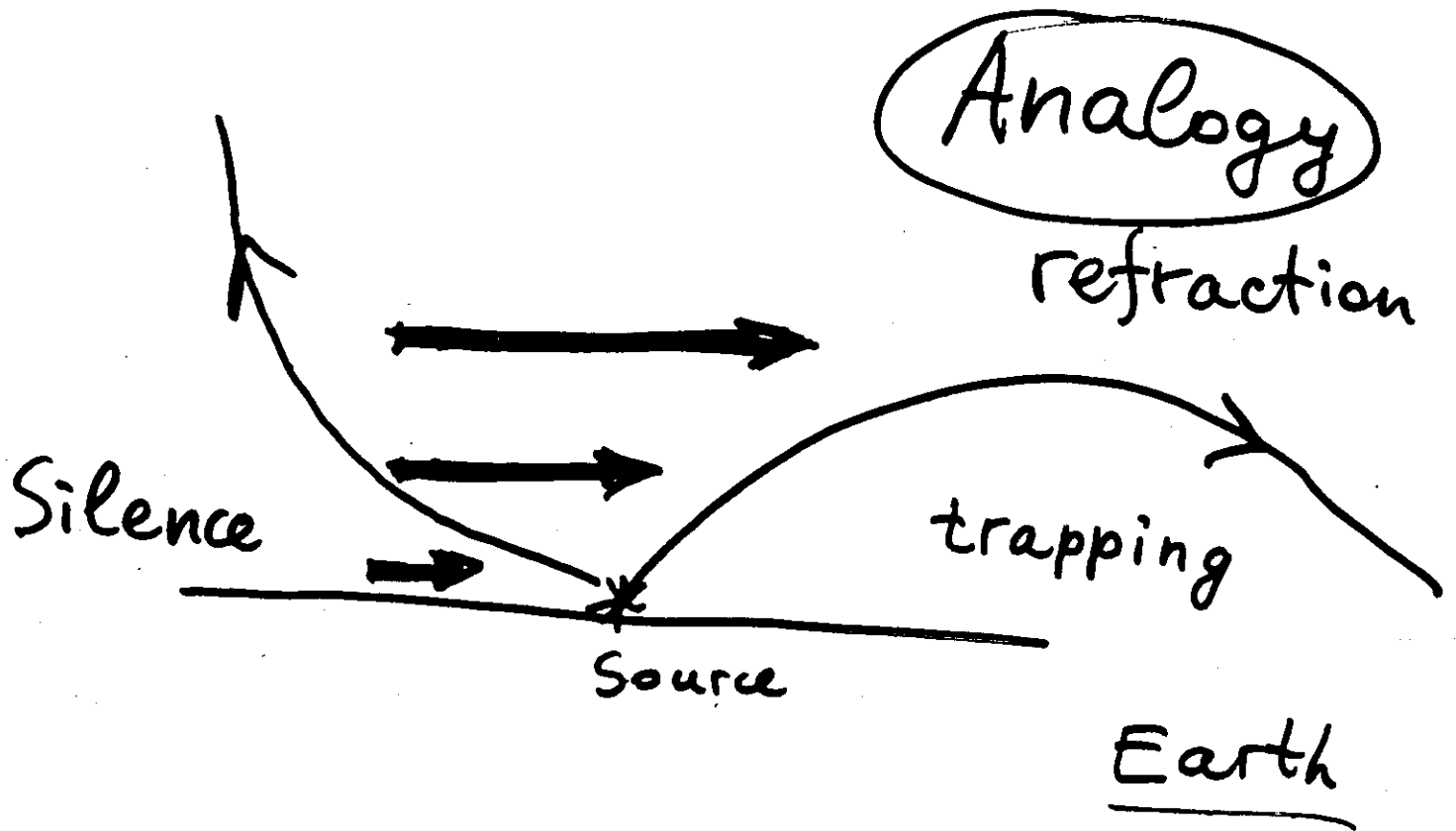
Limitations : 1) $\lambda \ll r$
 wave characteristic
 length scale

$\lambda \gtrsim r$ diffraction effects
(reverberation, smoothening
of the front shapes)

2) nonlinear effects

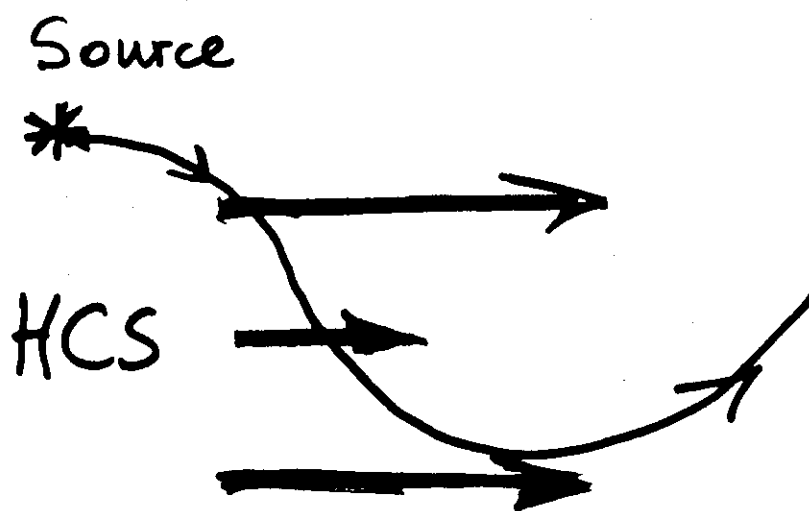
$$\delta \hat{S} \delta M \sim \hat{S} M$$

nonsteady state including waves



Where in the heliosphere?

HCS



Screening Silence Zone

Conclusions

- acoustogeometric (ray) approximation is useful in applications for heliospheric phenomena
- geometry of wave fronts in the heliosphere depends on the geometry of wave sources and the geometry of heliospheric inhomogeneities
- more careful studies are needed for a better understanding of real geometry

Shock front geometry description

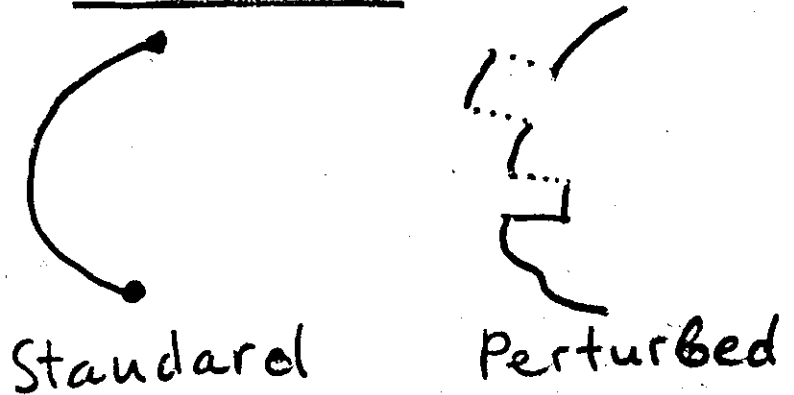
Global properties : Topology \rightarrow
connectivity parameters
one-connected

Local properties : Standard differential geometry
approach

Accuracy: I order II order

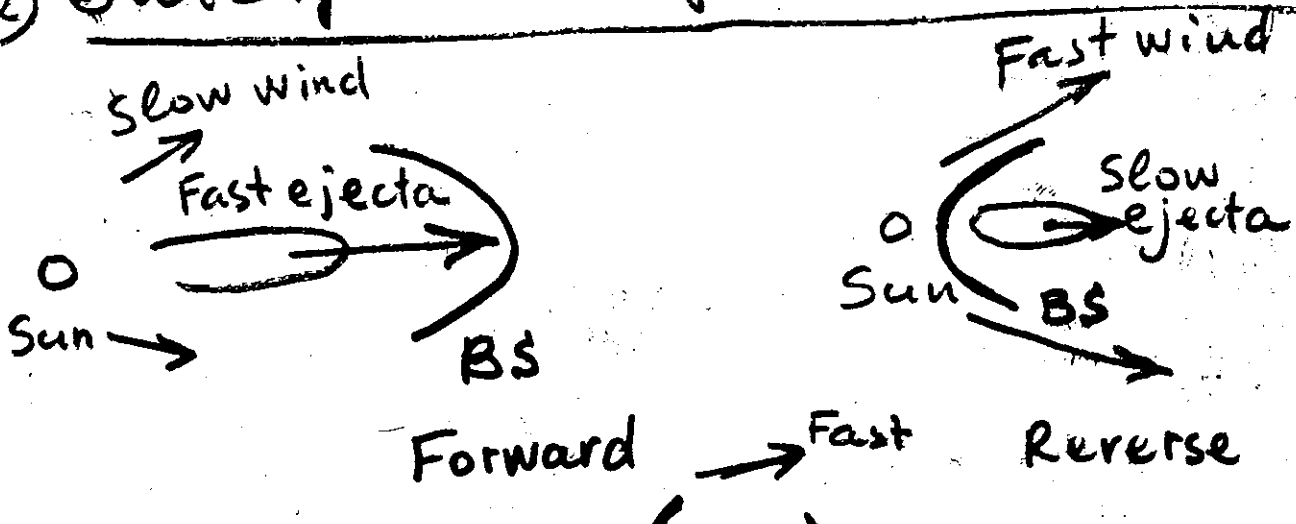
Higher order
Flattening
points

Examples : ① Bow shock (MP)



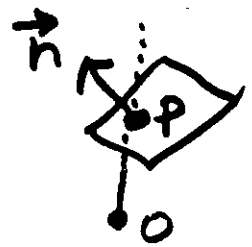
$\Delta t \ll \tau_{\text{formation}}$

② Interplanetary shocks (discontinuity)



Ist order approximation:

Tangential } planes
crossing



$$\Phi(x, y, z) = Gx + Hy + Iz + K = 0$$

3 numbers are necessary and sufficient to describe the plane:

$G/K, H/K, I/K$, for example:

- 1) The distance to the observer, O_P
- 2) Two angles - unit normal vector \vec{n} .

IInd order approximation:

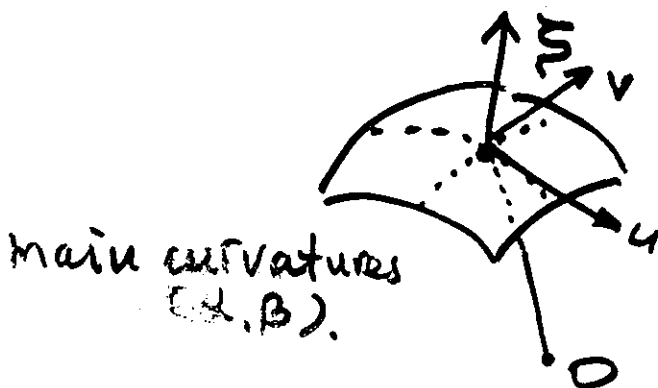
$$\Phi(x, y, z) = Ax^2 + By^2 + Cz^2 + Dxy + Exz + Fyz + Gx + Hy + Iz + K = 0$$

ϵ

Main axes

$$\xi = \alpha u^2 + \beta v^2$$

local coordinates (ξ, u, v)



Points:

$\alpha\beta > 0$ elliptic

$\alpha\beta < 0$ hyperbolic

$\alpha\beta = 0$ cylindric

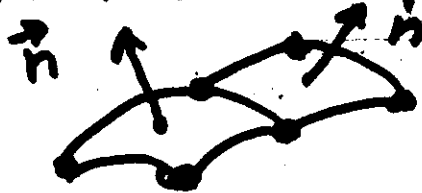
($\alpha \neq 0$ or $\beta \neq 0$)
 $\alpha = \beta = 0$ flattening

8 numbers are sufficient:

For example:

1) d, β \oplus 6 numbers to fix
a position : one point (3 numbers)
 \oplus 3 Euler's angles

Fox & Pratt : cubic splines, grids



"surface design" for "aviation engineering"

3 s/c are necessary and
sufficient to reconstruct the accom-
panying paraboloid for fixed or
"frozen" fronts $(\vec{r} = \vec{r}_i + \vec{v}(t_i - t_0))$

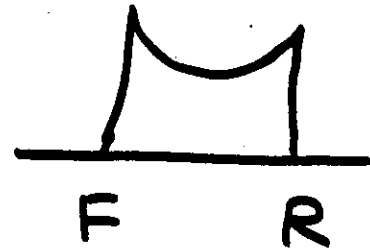
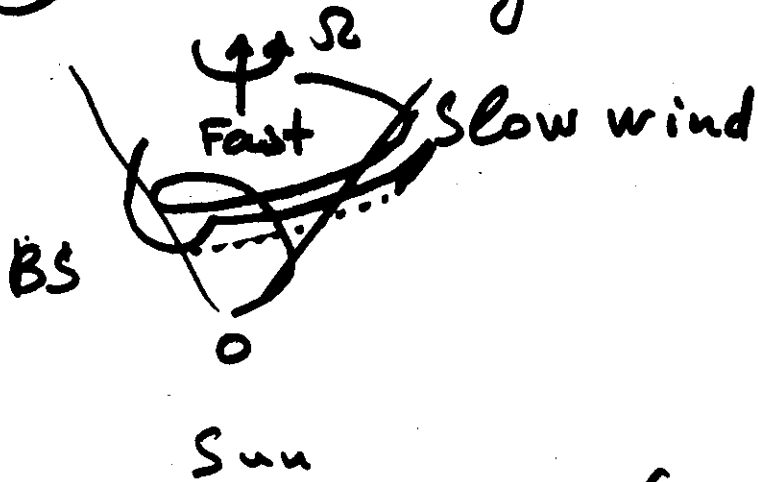
Correctness of the problem:

- the solution exists
- unique / single
- stable against perturbations

Overdetermined systems:

$$n_i(\vec{r}) \approx n_i(\vec{r}_0) + \frac{\partial n_i}{\partial r_k} (r_k - r_{k0}) + \dots$$

③ Corotating shocks



1) Conical axis

2) FR - pairs \equiv



\equiv one-connected surface (BS) which is crossed twice due to rotation.

3) paraboloid around conical axis.

Conclusions

1. The local shock front geometry is represented in the regular elliptic, cylindric or hyperbolic points by the accompanying paraboloid with the second order accuracy as compared to linear interpolations by tangential or crossing planes.
2. As a rule (with rare exceptions) 3 s/c are necessary and sufficient to characterize the local normal and the curvature tensor of the front surface at the given position (8 numbers inside the correlation volume).
3. Additional ($n > 3$) s/c inside the correlation volume allow to determine the higher order terms.
4. Local measurements outside the space-time correlation region combined with the remote sensing methods are needed to reconstruct the global geometry and topology (connectivity) of the surface.

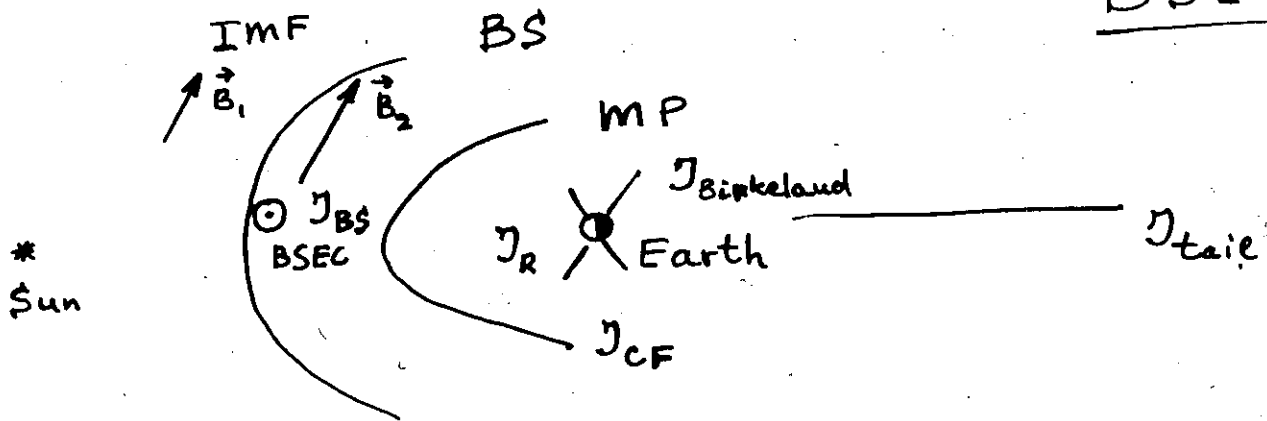
Bow shock associated electric currents in the magnetosphere and ionosphere

I.S. Veselovsky

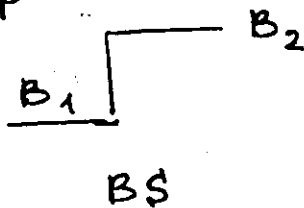
Institute of Nuclear Physics
Moscow State University
119899 Moscow Russia

Abstract. Bow shock electric currents (BSEC) are considered as a part of the unified heliosphere - magnetosphere - ionosphere current system. BSEC are generated locally by the jump conditions at the shock. They are highly variable and depend on the IMF orientation and Mach (M , M_s) numbers of the flow. BSEC are position dependent along the shock front and are strongest in the subsonic part near the places with the quasiperpendicular shock geometry and weaker at the flanks. Field aligned currents appear which are partially diverted into magnetosphere.

BSEC



Jump conditions:

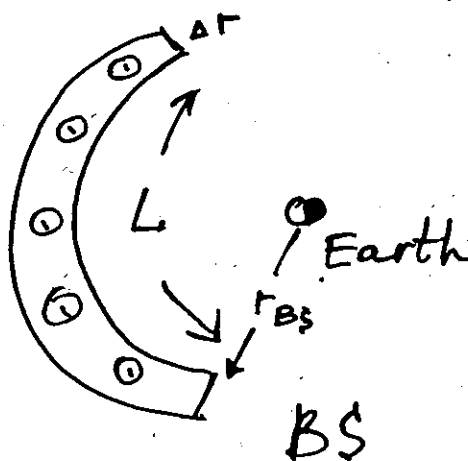


$$\Delta B \sim B_2 - B_1 \sim 10 \text{ nT}$$

$$\vec{j} = \frac{c}{4\pi} [\text{rot } \vec{B}]$$

$$J_{BS} \approx \int j dS \sim \frac{c}{4\pi} \Delta B L$$

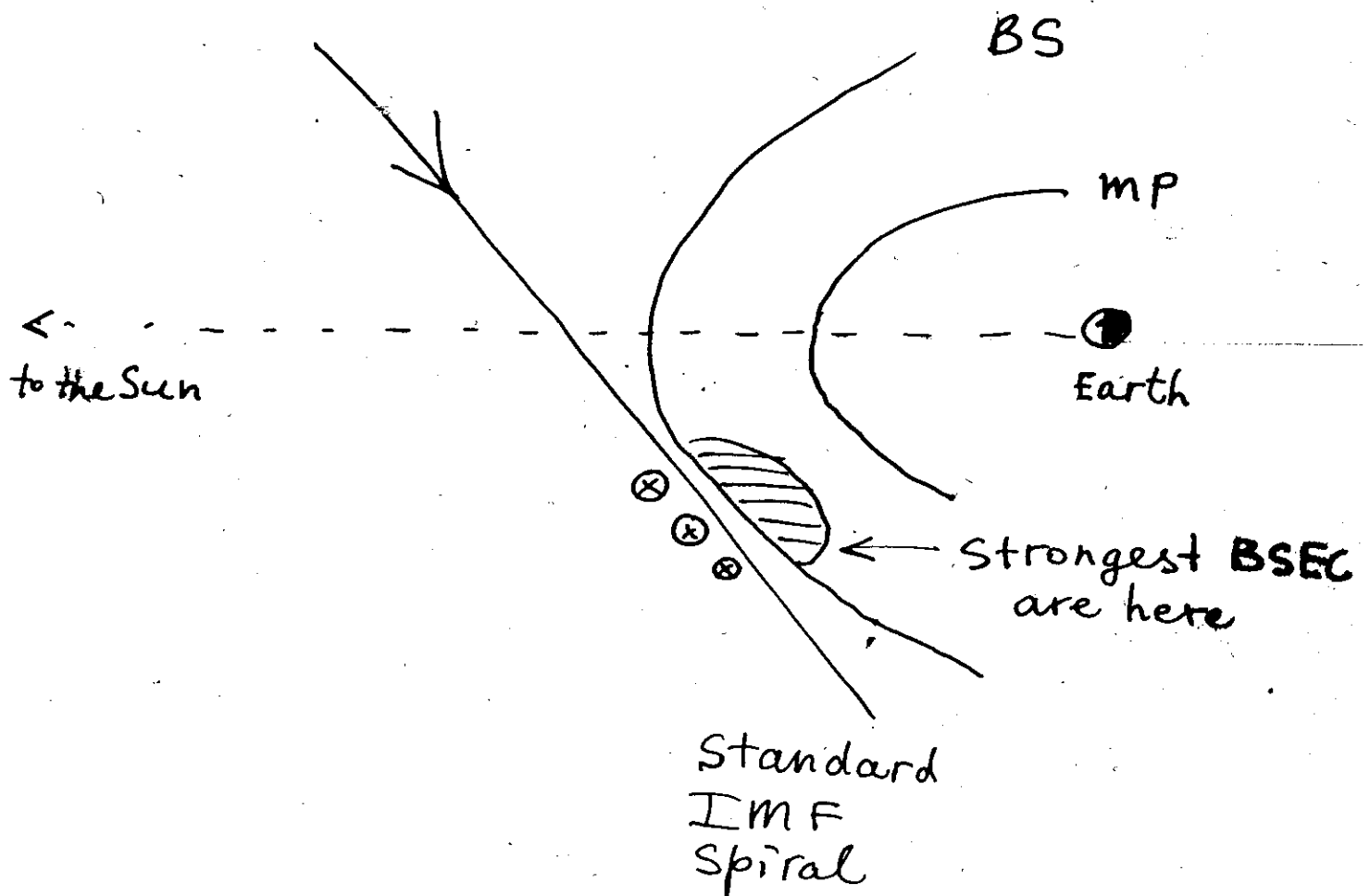
$$L \sim \pi r_{BS} \sim 4 \cdot 10^8 \text{ cm}$$



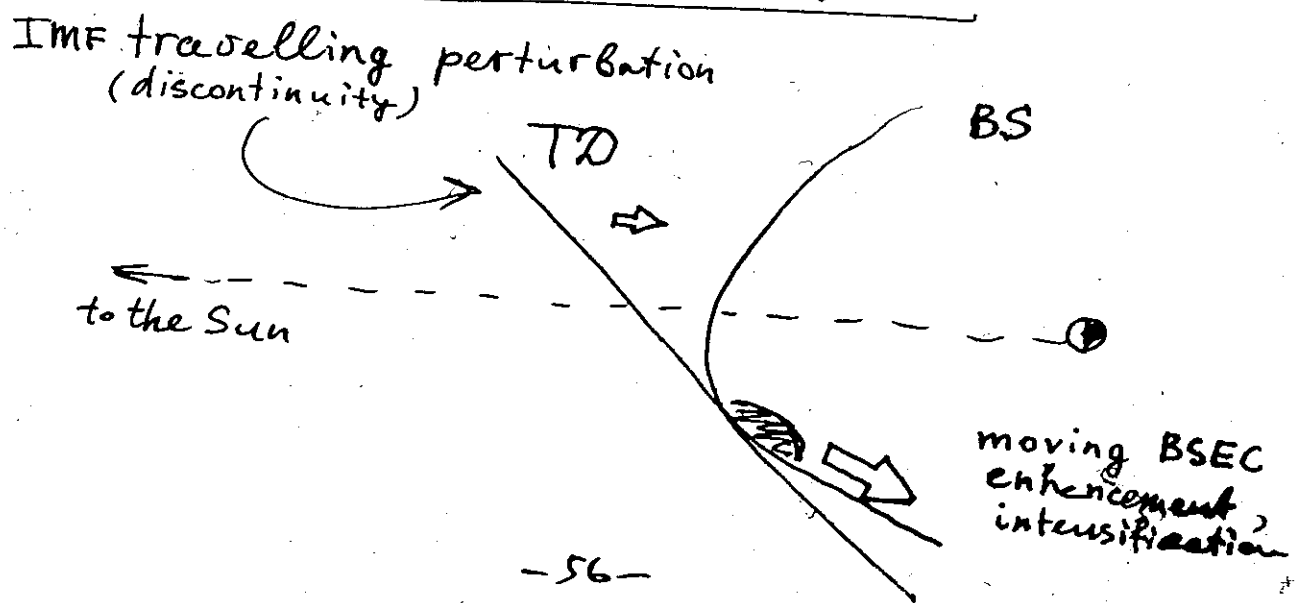
$$J_{BS} \sim 2 \text{ MA}$$

- the strength of BSEC depends on the IMF, m , m_A and position on BS.
 - the direction is determined by the IMF orientation and position on BS.
- because of this: strong variations of BSEC; t , r , with time, position and IMF

Stationary case



Nonstationary case



Conclusions:

~~=====~~ BSEC represents one of the more sensitive elements of the global near Earth's effective electrical circuit to the variations of the IMF directions and magnitude.

~~=====~~ Field aligned currents and vortices in the flow are generated on the bow shock.

BSEC are not closed on the bow shock surface

OPEN, CLOSED AND INTERMITTENT MAGNETIC STRUCTURES IN THE SOLAR CORONA AND THEIR HELIOSPHERIC IMPRINTS DURING THE SOLAR CYCLE

I.S.Veselovsky

*Institute of Nuclear Physics, Moscow State University, Moscow
119899, Russia*

ABSTRACT

A short account of theoretical and observational studies is presented supporting the ideas about complicated topological properties of the coronal and heliospheric magnetic fields and their changes during the solar cycle. The analogy is marked between the non-linear solar cycle behaviour and recursive magnetic phase transitions from more ordered (solar minima) to disordered (solar maxima) nonequilibrium states.

INTRODUCTION

The purpose of this paper is twofold. First of all, theoretical models are discussed, which show explicitly open, semi-open and closed magnetic fluxes. Secondly, their suggested manifestations are indicated in the solar wind and galactic cosmic ray data during the solar cycles 20-22. A short account of our recent works is presented.

THEORETICAL CONSIDERATIONS IMPLICATIONS

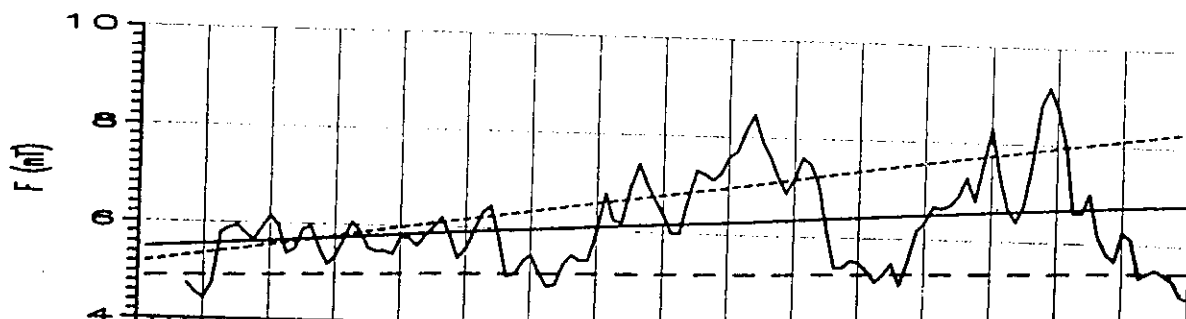
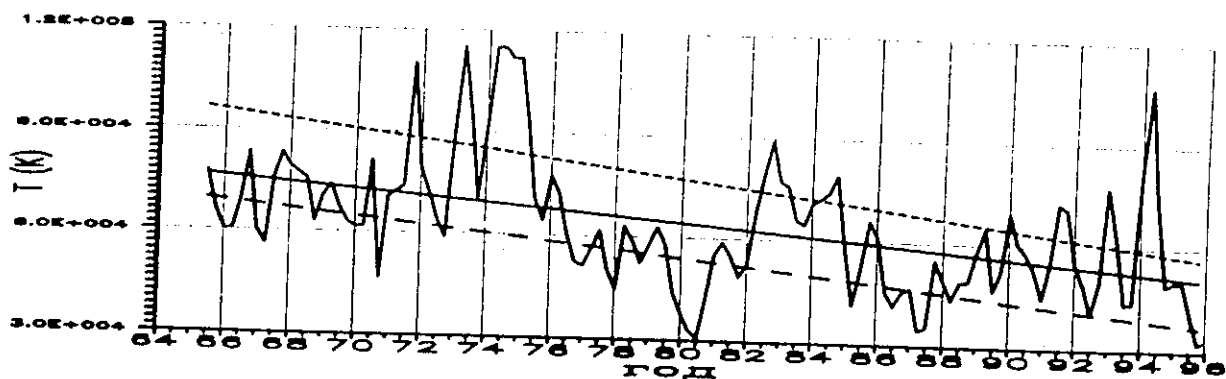
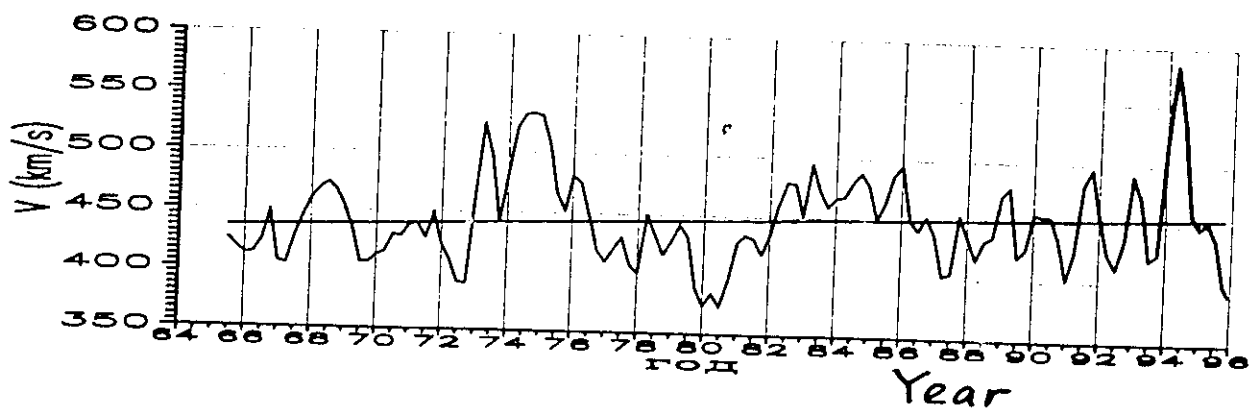
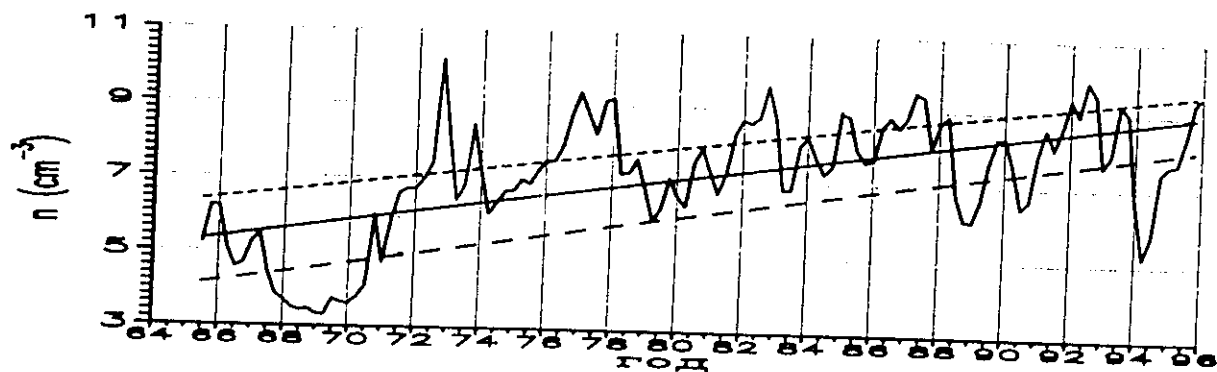
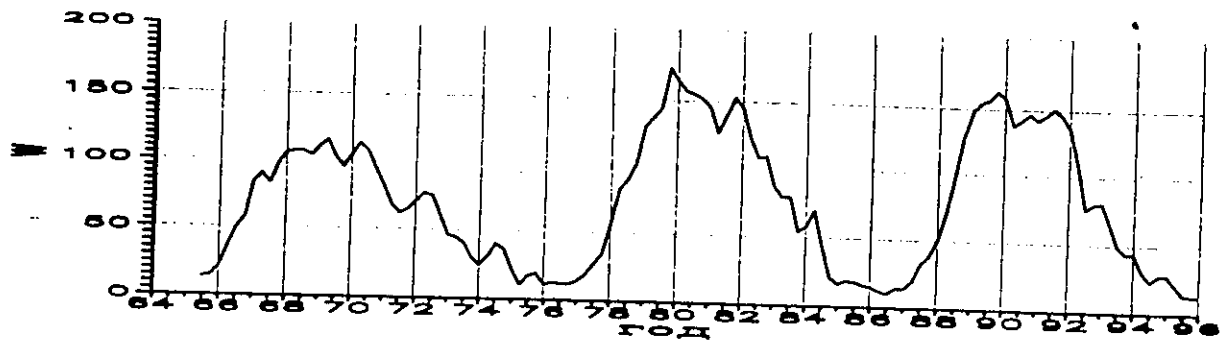
ISCS meeting, Nagoya, Japan, July 11, 1998

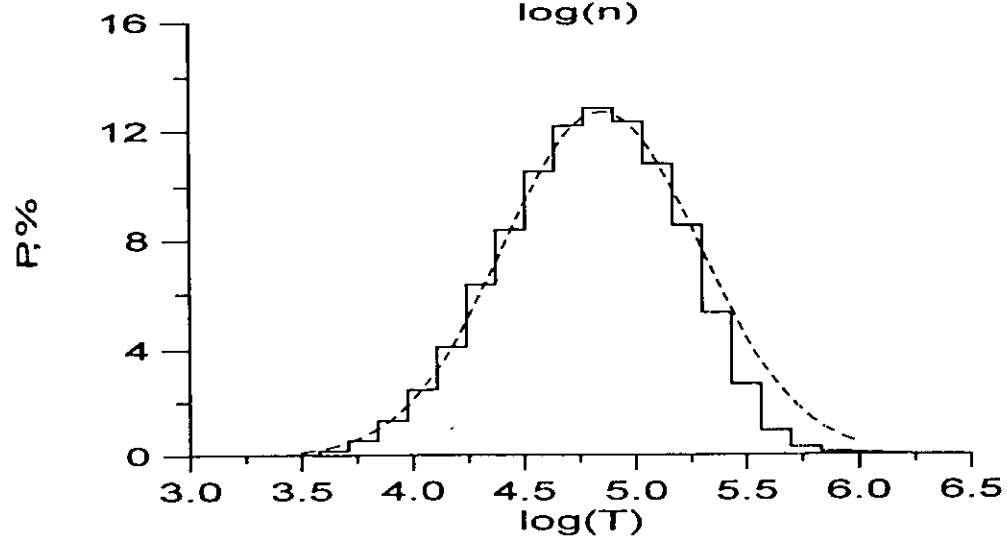
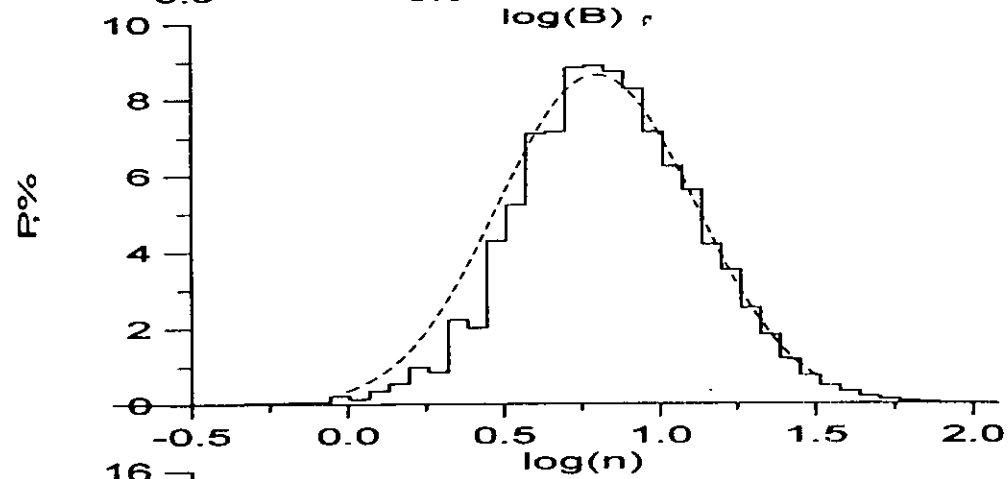
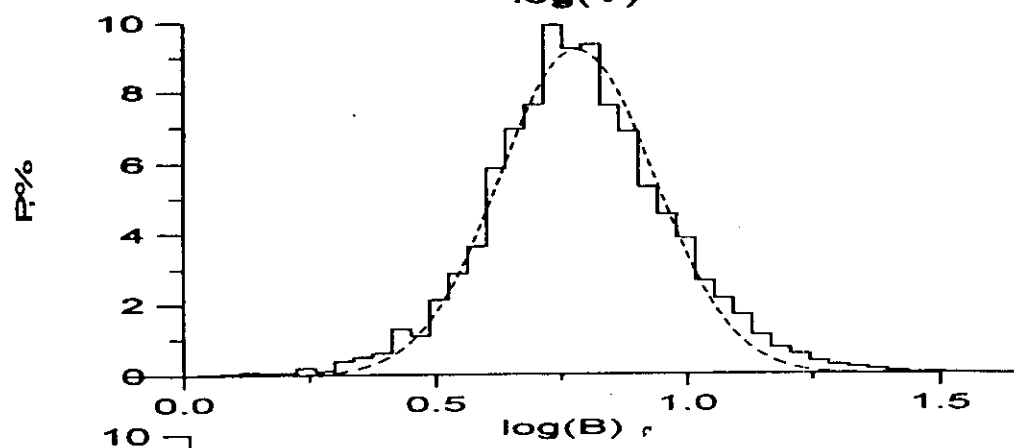
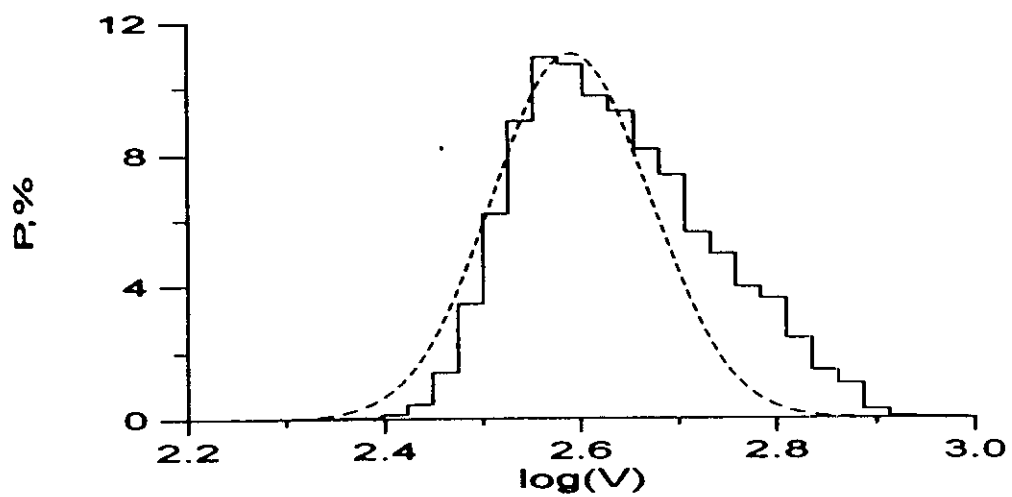
IMPLICATIONS

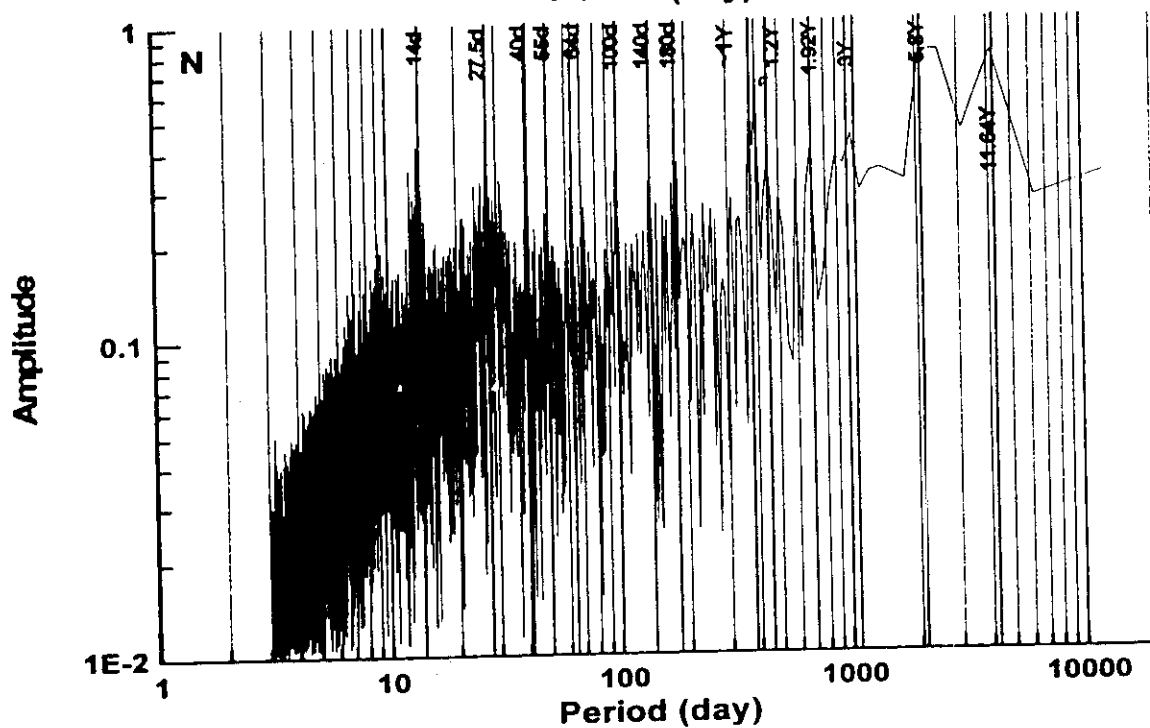
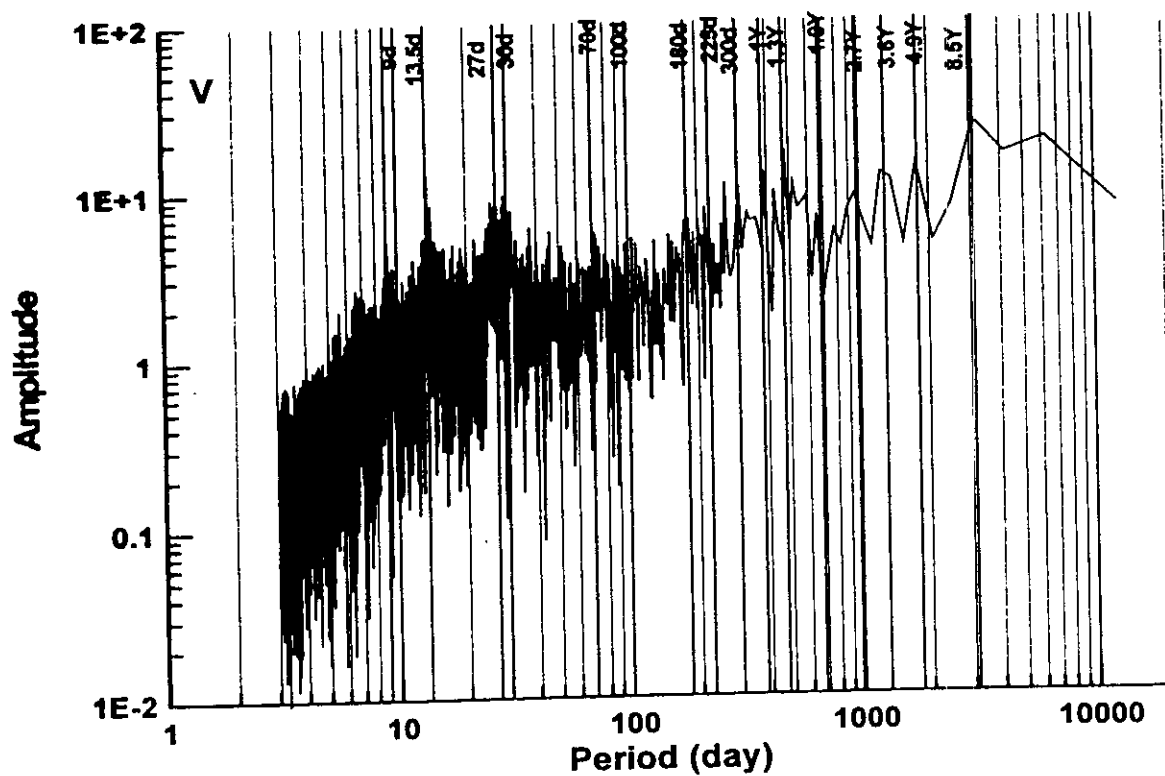
The observed and expected characteristics of the three-dimensional heliospheric magnetic fields near solar minima and at solar maxima were discussed in the literature (Balogh, 1996).

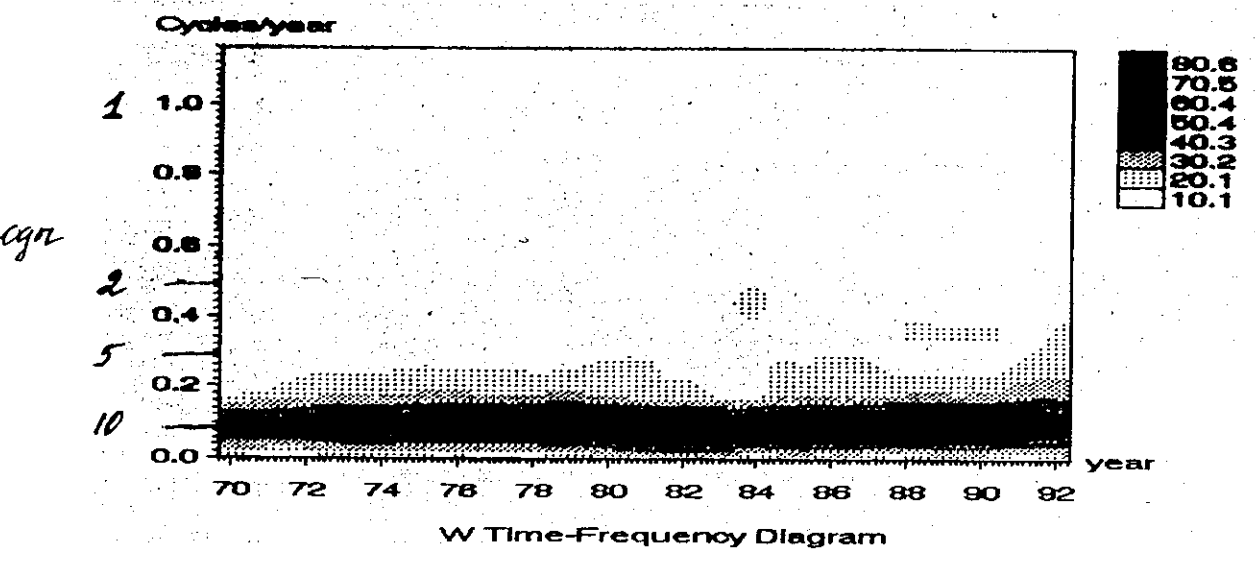
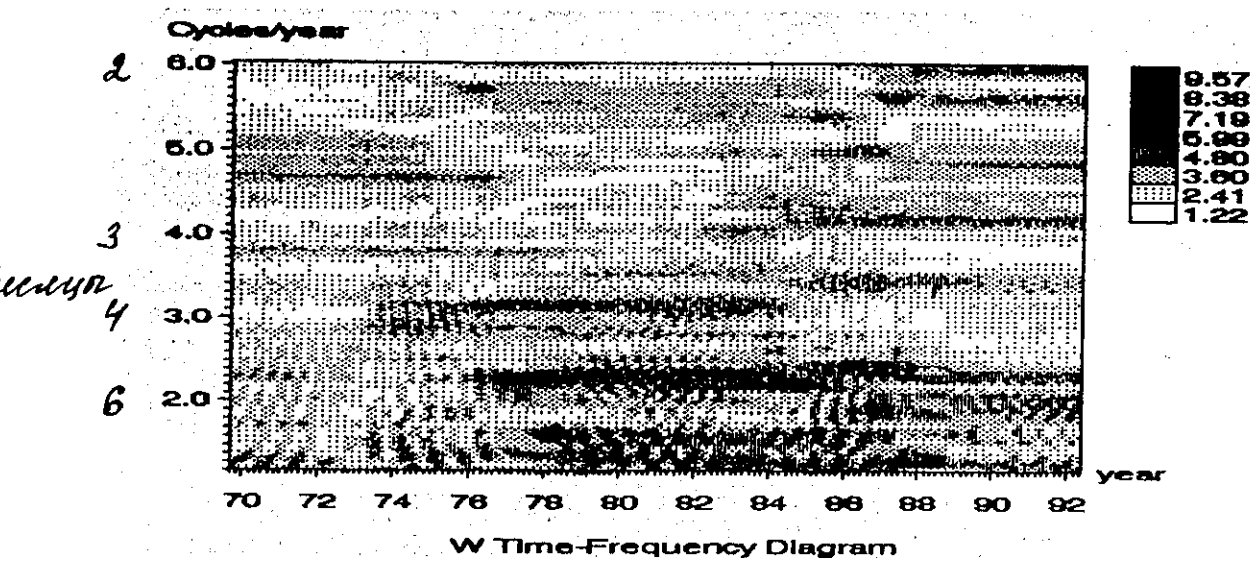
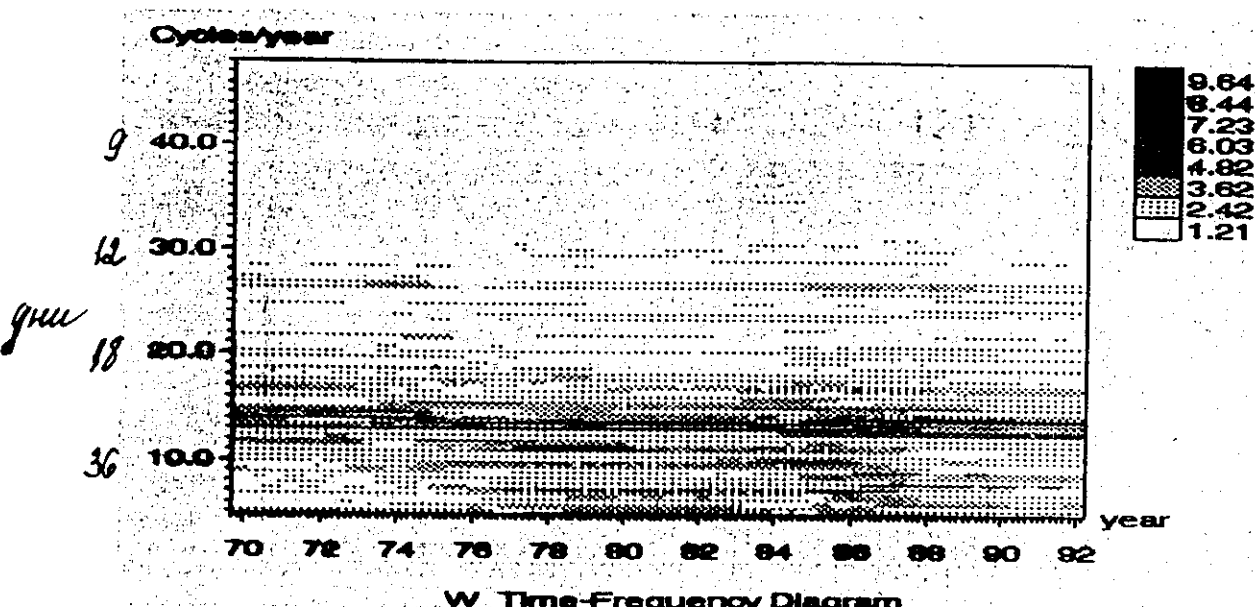
Considering our theoretical and observational grounds we are able to make several additional speculations about the solar cycle manifestations in the heliospheric magnetic fields in three dimensions:

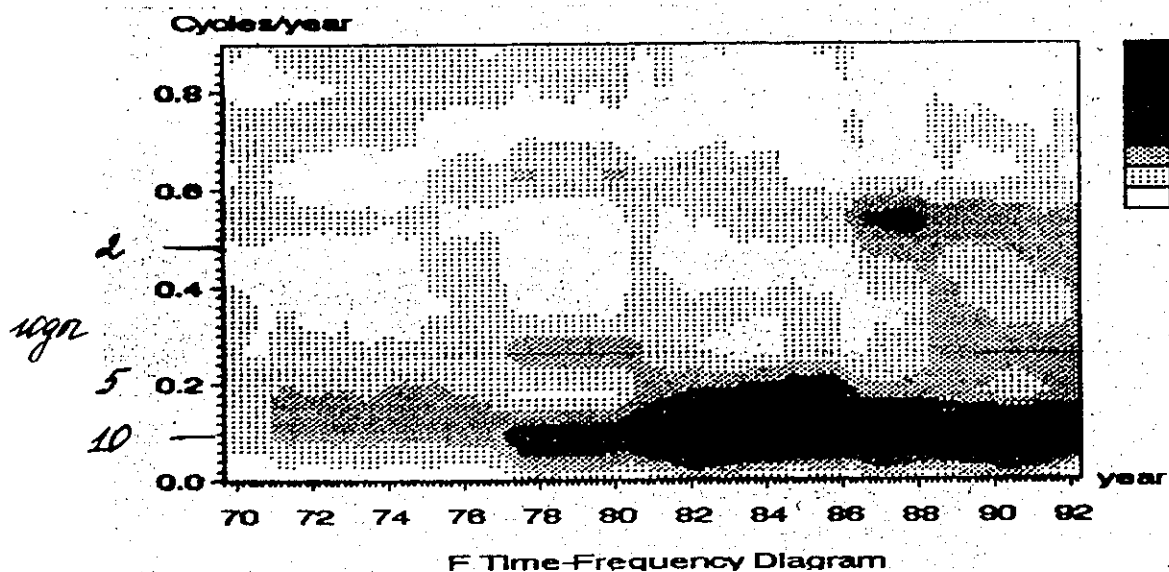
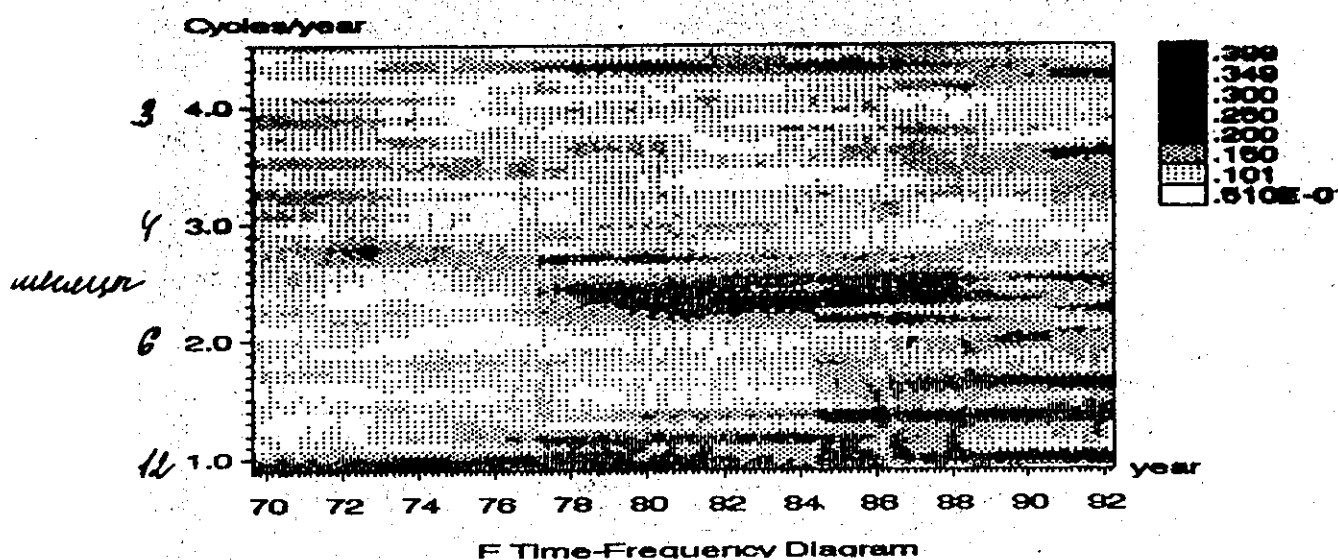
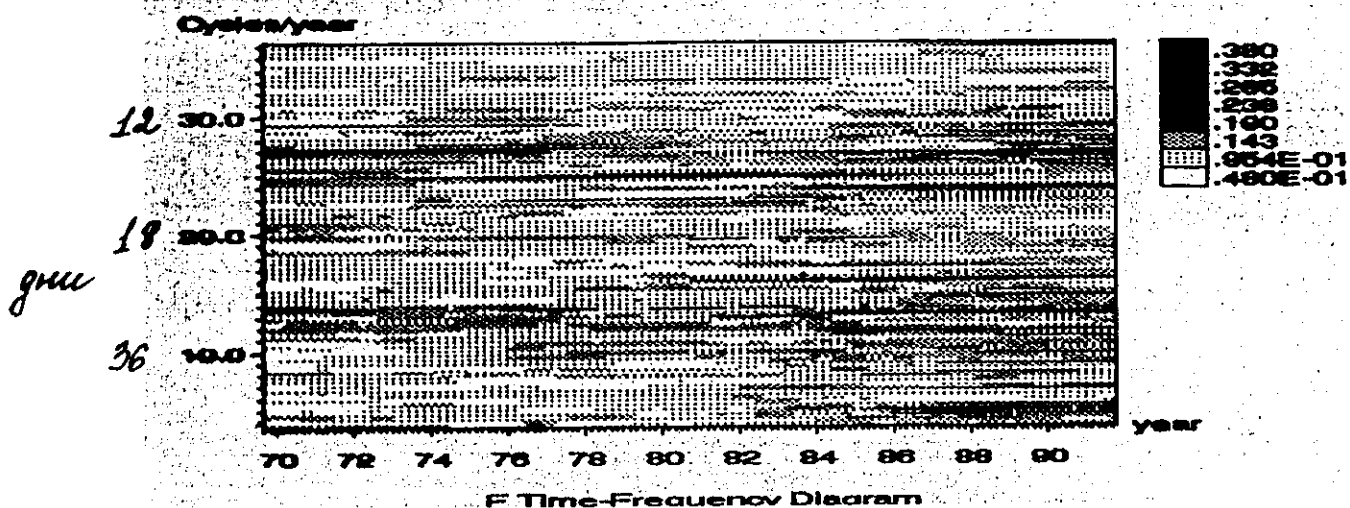
- 1) The overall magnetic field in the heliosphere at solar maxima should be higher than at solar minima by a factor of about 1.5.
- 2) Nonstationary magnetic fields (transients, magnetic clouds and filaments, shocks, different waves and discontinuities) are obviously more often and several times stronger during solar maxima. Nevertheless, the remaining quasi-stationary heliospheric field detrended from these strong nonstationary perturbations should be well organised by the heliospheric current sheet, which is inclined, corrugated and may be sometimes multiple or not one-connected due to the long-term and large-scale solar activity.
- 3) The natural demarcation between quasi-stationary and nonstationary heliospheric structures is given by the dimensionless Strouhal numbers $S = \frac{Vt}{\ell}$, where ℓ and t are characteristic space-time scales, V is the solar wind velocity.
- 4) The strength of the heliospheric current sheet and the corresponding radial magnetic fields are expected to be higher at solar maximum. The radial component of the quasi-stationary magnetic field outside (broader) current sheet regions should be roughly constant in its absolute value at the given sphere around the Sun.
- 5) Semi-open magnetic fluxes dominate in the inner heliosphere during solar minima, especially at high latitudes. Closed and intermittent magnetic configurations are more numerous near the Sun especially at maxima and near the heliospheric current sheet. The quantitative proportions are to be determined by observations.
- 6) A rapid transformation from solar minima to solar maxima and slower decay after maxima to minima could be associated with the underlying non-linear dynamics analogous to the recursive phase transitions in open systems out of the equilibrium. Corresponding models are under investigation and will be communicated separately.

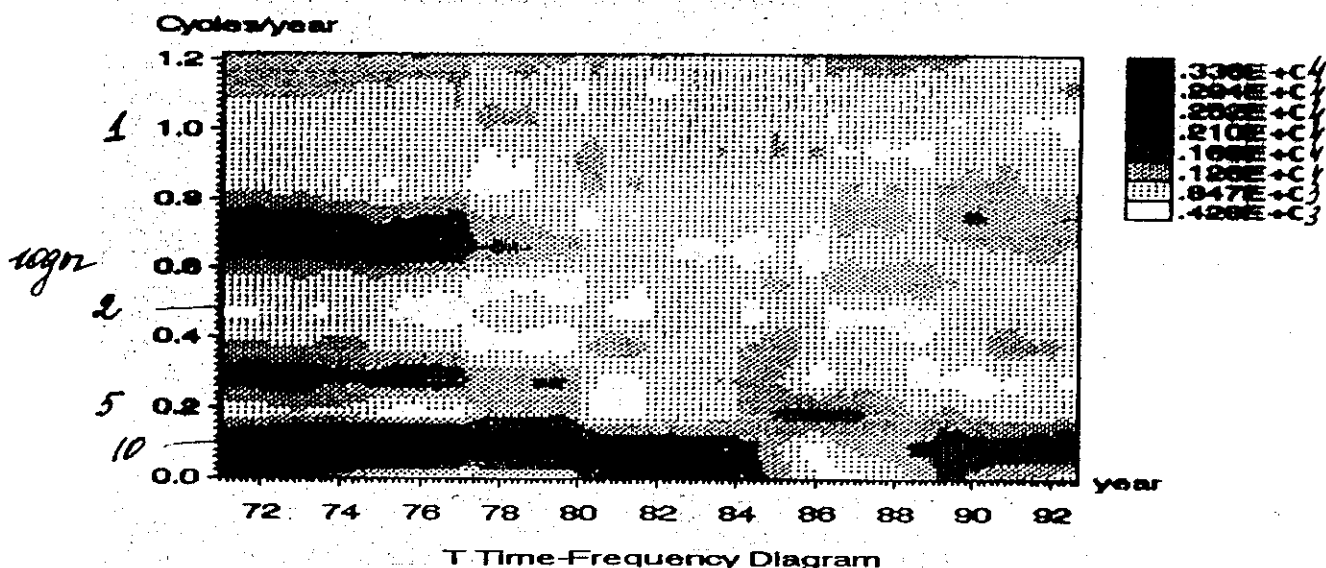
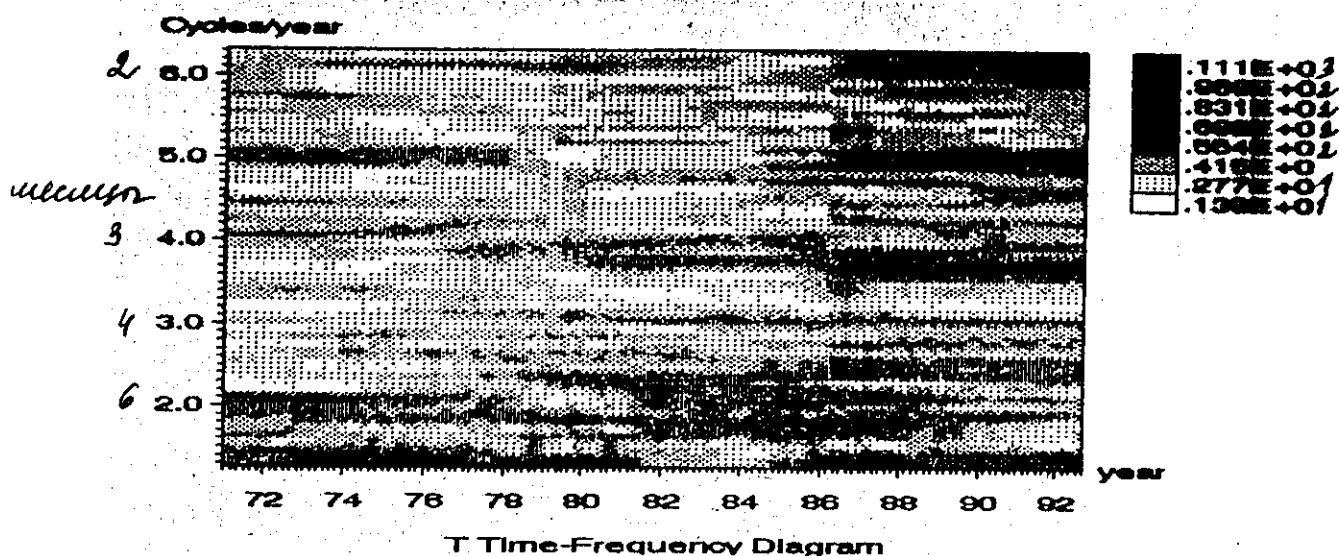
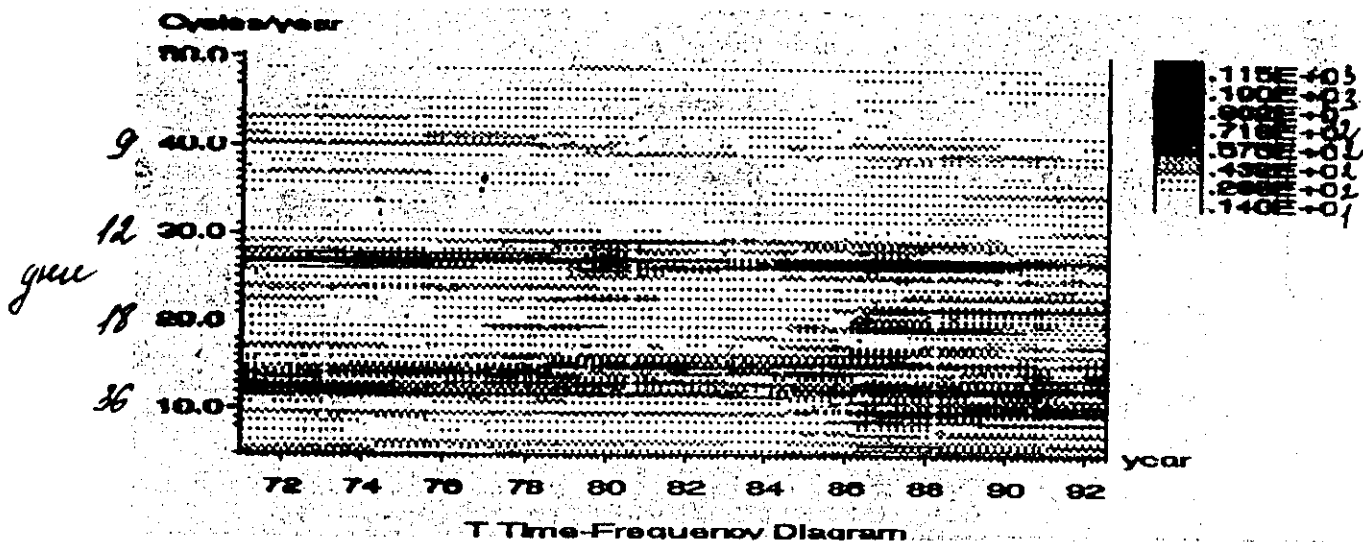












W Wavelet Transform (Symmetric Haar Transform)

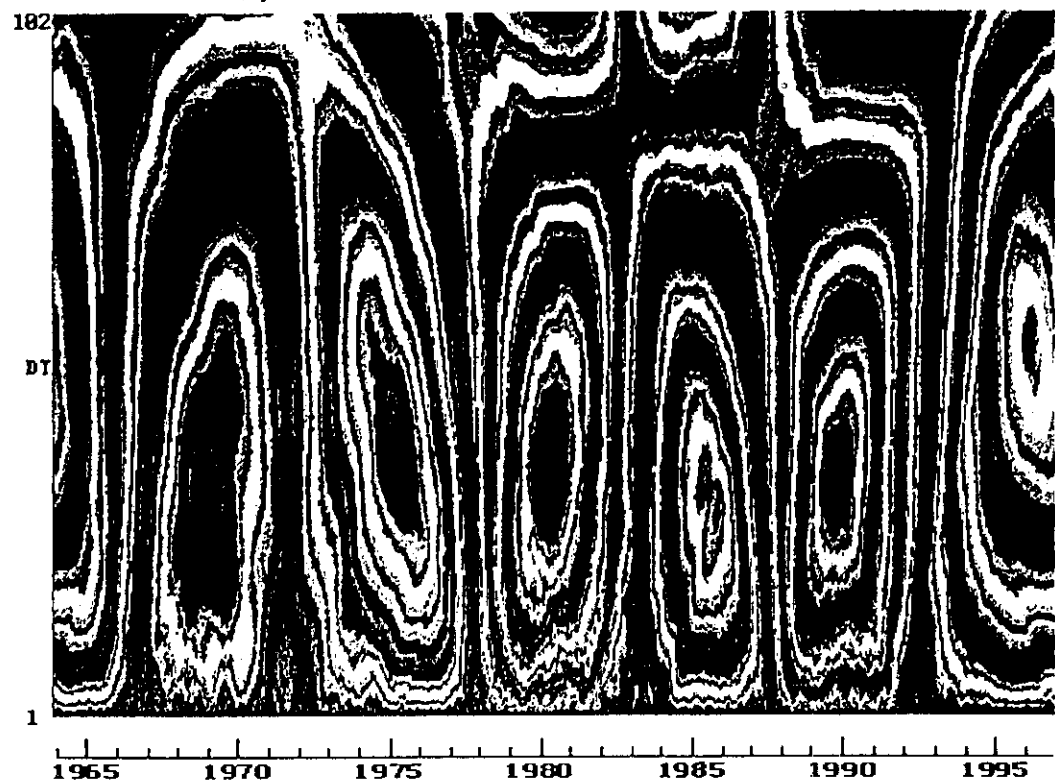


Рисунок 5а. Вейвлетный портрет для чисел Вольфа.

Symmetric Haar Transform

FWT.DAT

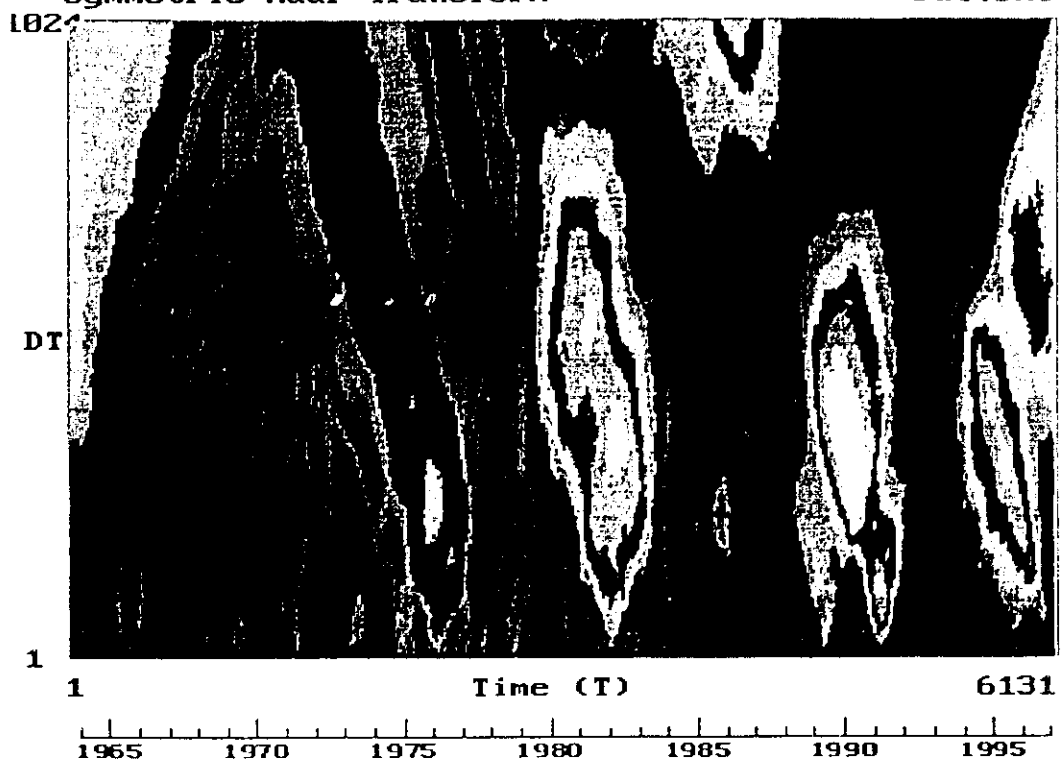


Рисунок 5б. Вейвлетный портрет для модуля магнитного поля.

Conclusions.

- 1) Solar wind and interplanetary magnetic field are remarkably variable at the Earth's position in the heliosphere over the whole time scale range under investigation from 1 hour up to 30 years corresponding to the frequency range $\omega = 1.7 \cdot 10^{-3} \div 6.6 \cdot 10^{-9} \text{ s}^{-1}$. These variations deserve more attentive investigations.
- 2) Statistical distributions of main heliospheric parameters are broad and show log-normal cores in many cases, but significant deviations are noted for all parameters. Deviations from purely Gaussian functions show both random and regular manifestations in the heliosphere. The turbulence in the heliosphere is not fully developed. It is intermittent in space and time because of the presence of convective and propagating structures.
- 3) Correlations between different parameters are seen in several instances, but the level of the coherent variations is rather low as a rule, especially for long-term variations.
- 4) General trends definitely exist in the heliospheric parameters during the last three solar cycles № 20, 21, and 22. These trends may be tentatively interpreted as parts of the solar and heliospheric cycle with the duration 60 - 70 years.
- 5) Specific solar cycle variations are found for all heliospheric parameters to be of the order of several 10^{-1} . They are confirmed for the interplanetary magnetic field, the solar wind velocity and the dynamic pressure at the Earth's position in the heliosphere.
- 6) Temperature shows distinct solar cycle variations well correlated with the velocity.
- 7) Variations of the mean solar wind density during the solar cycle may be described roughly as follows. Relatively low one - year averages are observed for periods of time about 1-2 years just before solar minima and during solar maxima. For the same solar cycles, relatively high mean densities appear 1-2 years before and after solar maxima. As a result, the five-year wave dominates over the eleven-year wave in the solar cycle mean density variations.
- 8) General trends and solar cycle variations of the mean heliospheric parameters are clearly manifested in the geomagnetic activity indices.
- 9) The observed long-term variations of the heliospheric parameters and their phase relations as well as statistical characteristics does not contradict the concepts of the solar wind sources from magnetically open, closed and intermittent structures on the Sun.

<http://alpha.npi.msu.su/~alla>

